

1 **Triple oxygen isotope evidence for the pathway of nitrous oxide**  
2 **production in a forested soil with increased emission on rainy days**

3

4 Weitian Ding<sup>1</sup>, Urumu Tsunogai<sup>1</sup>, Tianzheng Huang<sup>1</sup>, Takashi Sambuichi<sup>1</sup>, Wenhua  
5 Ruan<sup>1</sup>, Masanori Ito<sup>1</sup>, Hao Xu<sup>1</sup>, Yongwon Kim<sup>2</sup>, Fumiko Nakagawa<sup>1</sup>

6

7 <sup>1</sup>Graduate School of Environmental Studies, Nagoya University, Furo-cho, Chikusa-ku,  
8 Nagoya 464-8601, Japan

9 <sup>2</sup>International Arctic Research Center, University of Alaska Fairbanks, Fairbanks, Alaska  
10 99775-7320, USA

11

12 Corresponding author: Weitian Ding

13 Email: dwt530754556@gmail.com

14

## Abstract

Continuous increases in atmospheric nitrous oxide ( $\text{N}_2\text{O}$ ) concentrations are a global concern. Both nitrification and denitrification are the major pathways of  $\text{N}_2\text{O}$  production in soil, one of the most important sources of tropospheric  $\text{N}_2\text{O}$ . The  $^{17}\text{O}$  excess ( $\Delta^{17}\text{O}$ ) of  $\text{N}_2\text{O}$  can be a promising signature for identifying the main pathway of  $\text{N}_2\text{O}$  production in soil. However, reports on  $\Delta^{17}\text{O}$  are limited. Thus, we determined temporal variations in the  $\Delta^{17}\text{O}$  of  $\text{N}_2\text{O}$  emitted from forested soil for more than one year and that of soil nitrite ( $\text{NO}_2^-$ ), which is a possible source of O atoms in  $\text{N}_2\text{O}$ . We found that  $\text{N}_2\text{O}$  emitted from the soil exhibited significantly higher  $\Delta^{17}\text{O}$  values on rainy days ( $+0.12 \pm 0.13 \text{ ‰}$ ) than on fine days ( $-0.30 \pm 0.09 \text{ ‰}$ ), and the emission flux of  $\text{N}_2\text{O}$  was significantly higher on rainy days ( $38.8 \pm 28.0 \text{ } \mu\text{g N m}^{-2} \text{ h}^{-1}$ ) than on fine days ( $3.8 \pm 3.1 \text{ } \mu\text{g N m}^{-2} \text{ h}^{-1}$ ). Because the  $\Delta^{17}\text{O}$  values of  $\text{N}_2\text{O}$  emitted on rainy and fine days were close to those of soil  $\text{NO}_2^-$  ( $+0.23 \pm 0.12 \text{ ‰}$ ) and  $\text{O}_2$  ( $-0.44 \text{ ‰}$ ), we concluded that although nitrification was the main pathway of  $\text{N}_2\text{O}$  production in the soil on fine days, denitrification became active on rainy days, resulting in a significant increase in the emission flux of  $\text{N}_2\text{O}$ . This study reveals that the main pathway of  $\text{N}_2\text{O}$  production can be identified by precisely determining the  $\Delta^{17}\text{O}$  values of  $\text{N}_2\text{O}$  emission from soil and by comparing the  $\Delta^{17}\text{O}$  values with those of  $\text{NO}_2^-$ ,  $\text{O}_2$ , and  $\text{H}_2\text{O}$  in the soil.

## 1. Introduction

Nitrous oxide ( $\text{N}_2\text{O}$ ) is a strong greenhouse gas and an essential substance in stratospheric ozone depletion (Dickinson and Cicerone, 1986). Since pre-industrial times, the atmospheric  $\text{N}_2\text{O}$  level has increased by 24 % to 335.8 ppb, with an average growth rate of  $1.05 \text{ ppb yr}^{-1}$  in the last decade (WMO, 2023). Terrestrial soils account for ~60 % of total  $\text{N}_2\text{O}$  emissions (Tian et al., 2020). Therefore, better knowledge of the pathways of  $\text{N}_2\text{O}$  production in soils is required to establish mitigation measures.

Both nitrification and denitrification are representative microbial pathways of  $\text{N}_2\text{O}$  production in soils (Wrage et al., 2001). Nitrification is the oxidation of ammonium ( $\text{NH}_4^+$ ) to nitrate ( $\text{NO}_3^-$ ) via aerobic microbial activity, during which  $\text{N}_2\text{O}$  is produced as a byproduct of hydroxylamine ( $\text{NH}_2\text{OH}$ ) oxidation to nitrite ( $\text{NO}_2^-$ ), while denitrification is the reduction of  $\text{NO}_3^-$  to  $\text{NO}_2^-$  and then to  $\text{N}_2\text{O}$  which is further reduced to nitrogen ( $\text{N}_2$ ) via facultative anaerobes (Figure 1). Soil conditions such as moisture content,  $\text{O}_2$  availability (Bateman and Baggs, 2005; Zhu et al., 2013), temperature (Luo et al., 2007), and fertilizer types (Zhu et al., 2013) have been proposed as parameters to determine the pathways of  $\text{N}_2\text{O}$  production in soils.

Techniques such as acetylene blockage (Balderston et al., 1976; Lin et al., 2019), artificial isotope tracers ( $^{15}\text{N}$  and  $^{18}\text{O}$ ) (Mulvaney and Kurtz, 1982; Wrage et al., 2004), and natural stable isotopes (Toyoda et al., 2013; Yu et al., 2020) are conventionally used to identify the pathways of  $\text{N}_2\text{O}$  production via nitrification and denitrification. Both acetylene blockage and artificial isotope tracers are mostly performed in laboratory (*in vitro*) incubations because they are costly, complicated, and time-consuming in field research. Natural stable isotopes such as  $\delta^{15}\text{N}$ ,  $\delta^{18}\text{O}$ , and SP ( $^{15}\text{N}$  site preference) can be

used to identify the pathways of  $\text{N}_2\text{O}$  production in soils (Decock and Six, 2013; Toyoda et al., 2017; Verhoeven et al., 2019). However, further reduction of  $\text{N}_2\text{O}$  to  $\text{N}_2$  after the production of  $\text{N}_2\text{O}$  until emission from soil to air results in significant changes in the  $\delta^{15}\text{N}$ ,  $\delta^{18}\text{O}$ , and SP values of  $\text{N}_2\text{O}$  due to the fractionation of isotopes, which makes the identification process difficult (Ostrom et al., 2007).

Recent studies on the  $\Delta^{17}\text{O}$  value of  $\text{NO}_3^-$  (the definition detailed in Section 2.4) have reported that  $\Delta^{17}\text{O}$  is a useful natural signature for clarifying the complicated biogeochemical processes in terrestrial ecosystems (Ding et al., 2022, 2023, 2024; Michalski et al., 2004; Tsunogai et al., 2010). Although the values of  $\delta^{15}\text{N}$ ,  $\delta^{18}\text{O}$ , and SP can vary during various fractionation processes of isotopes within terrestrial ecosystems, the  $\Delta^{17}\text{O}$  value remains almost stable because possible variations in  $\delta^{17}\text{O}$  and  $\delta^{18}\text{O}$  values during the processes of biogeochemical isotope fractionation follow the relation of  $\delta^{17}\text{O} \approx 0.5 \delta^{18}\text{O}$ , which cancels out the variations in the  $\Delta^{17}\text{O}$  value (Young et al., 2002). Consequently, the mixing of the same oxygen compounds with different  $\Delta^{17}\text{O}$  values is the primary cause of variations in  $\Delta^{17}\text{O}$  values throughout the biogeochemical processes in terrestrial ecosystems.

Because  $\text{N}_2\text{O}$  produced through nitrification is a byproduct of the oxidation reaction between  $\text{NH}_4^+$  (to  $\text{NH}_2\text{OH}$ ) and  $\text{O}_2$ , the  $\Delta^{17}\text{O}$  value of  $\text{N}_2\text{O}$  produced through nitrification is expected to be close to that of tropospheric  $\text{O}_2$  (Figure 1) (Kool et al., 2007, 2011; Wrage et al., 2005), with previous studies reporting a  $\Delta^{17}\text{O}$  value of  $-0.44 \text{ ‰}$  (Sharp and Wostbrock, 2021). Conversely, the  $\Delta^{17}\text{O}$  value of  $\text{N}_2\text{O}$  produced through denitrification is expected to be close to that of  $\text{NO}_2^-$  (Figure 1) (Kool et al., 2007, 2011; Wankel et al., 2017; Wrage et al., 2005). Because O atoms in  $\text{NO}_2^-$  are derived from either soil  $\text{NO}_3^-$

( $\Delta^{17}\text{O}$  = from 0 to +20 ‰) or  $\text{H}_2\text{O}$  ( $\Delta^{17}\text{O}$  =  $+0.03 \pm 0.01$  ‰) (Hattori et al., 2019; Nakagawa et al., 2018; Uechi and Uemura, 2019), significant differences in  $\Delta^{17}\text{O}$  values between  $\text{N}_2\text{O}$  produced through nitrification and that produced through denitrification are expected if the additional contributions of O atoms derived from soil  $\text{H}_2\text{O}$  are insignificant in  $\text{N}_2\text{O}$  during the processes of  $\text{N}_2\text{O}$  production in soils through nitrification and denitrification (Figure 1) (Kool et al., 2007).

Previous studies have identified the elevated  $\Delta^{17}\text{O}$  values in atmospheric  $\text{N}_2\text{O}$  ( $\Delta^{17}\text{O} \approx +0.9$  ‰), observed in both stratospheric and tropospheric air (Cliff et al., 1999; Kaiser et al., 2003; Thiemens and Trogler, 1991). Komatsu et al. (2008) subsequently conducted the first  $\Delta^{17}\text{O}$  measurements of  $\text{N}_2\text{O}$  emitted from a soil to assess whether soil  $\text{N}_2\text{O}$  could be the source of elevated  $\Delta^{17}\text{O}$  values of atmospheric  $\text{N}_2\text{O}$ . However, the temporal variations of the  $\Delta^{17}\text{O}$  values for  $\text{N}_2\text{O}$  emitted from soil remain unknown. Besides, whether  $\Delta^{17}\text{O}$  values of  $\text{N}_2\text{O}$  can be used to identify the pathways of  $\text{N}_2\text{O}$  production in soils has not been discussed. Additionally, the advantages of  $\Delta^{17}\text{O}$  signature, relative to other natural stable isotopes, for identifying the pathways of  $\text{N}_2\text{O}$  production remain unclear. To address these, in this study, we measured precise  $\Delta^{17}\text{O}$  values for  $\text{N}_2\text{O}$  emitted from forested soil and those for  $\text{NO}_2^-$  in the soil. Additionally, we conducted similar observations in the same soil artificially fertilized with Chile saltpeter or urea to investigate the possible contributions of O atoms derived from soil  $\text{H}_2\text{O}$  in  $\text{N}_2\text{O}$  during  $\text{N}_2\text{O}$  production.

## 2. Methods

### 2.1 Study site

The study site was located in a secondary warm-temperate forest within an urban area (35°10'N, 136°58'E, Figure 2), approximately 50 m from the common building of the Graduate School of Environmental Studies at Nagoya University. The lowest, highest, and mean monthly temperatures recorded at the nearest meteorological station (Nagoya station) were 5.2 °C (in January), 28.9 °C (in July), and 18.5 °C, respectively, from April 2022 to July 2023. The annual mean precipitation was approximately 1800 mm. The soil stratum in the forested field possessed an approximate depth of 20 cm, characterized by a bulk density of 1.12 g/cm<sup>3</sup>. Details of the forest have been described in the previous study (Hiyama et al., 2005).

## **2.2 Sampling of N<sub>2</sub>O**

Samples of N<sub>2</sub>O emitted from the forested soil under natural conditions were collected 18 times (n = 18) from April 2022 to July 2023 in a field with an area of 5 m<sup>2</sup> (Figure 2b). Among the samples, 12 were collected on fine days, whereas 6 were collected on rainy days. A fine day is defined as a day without precipitation for 48 hours prior to the end of each sampling. The total precipitation within 12 h at the end of each sampling of the rainy days exceeded 12 mm.

The sampling of N<sub>2</sub>O emitted from the artificially fertilized soil was performed during a period of fine weather in three plots (1 m<sup>2</sup> for each located more than 5 m away from each other) within the same forested field, located approximately 3 m away from the plot where we conducted the sampling under natural conditions (Figures 2b and 2c). Either urea (CO(NH<sub>2</sub>)<sub>2</sub>, 46 % TN) or Chile saltpeter (KNO<sub>3</sub>, 14 % TN) was applied to two of the plots (U and CS plots) on 2023/7/16 at the same N amount of 250 kg N ha<sup>-1</sup>. Urea is a

synthetic N fertilizer (Sun & Hope Ltd., Japan), and Chile saltpeter (SQM Ltd., USA) contains  $\text{NO}_3^-$  with a high  $\Delta^{17}\text{O}$  value of +19 ‰ (determined through the internationally distributed isotope reference materials USGS-34 and USGS-35). The third plot was blank, meaning no fertilizer was added (NF plot). Sampling of  $\text{N}_2\text{O}$  from each plot was performed twice on days 2 and 6 after the addition of each fertilizer.

To precisely determine  $\Delta^{17}\text{O}$  of  $\text{N}_2\text{O}$ , more than 60 nmol of  $\text{N}_2\text{O}$  is required (Komatsu et al., 2008), which corresponds to more than 4 L of air containing  $\text{N}_2\text{O}$  at atmospheric concentrations. Accordingly, in this study, a flow chamber made of polypropylene with dimensions of 0.8 m  $\times$  0.3 m  $\times$  0.18 m was deployed onto the sampling site throughout each day of sampling (Figure S1). This chamber has an inlet and outlet port with an inner diameter of 1 cm. The outlet port was connected to an air pump using Tygon tubing, and the inlet port was open to ambient air. Using the air pump, the air in the chamber was taken into a 5-L aluminum bag, along with the gases emitted by the soil, as illustrated in Figure S1. The flow rate of the air pump was set at 100 ml/min throughout the deployment of the chamber; thus, each sampling lasted 45 min until 4.5 L of gas was collected into the aluminum bag. Each gas sampling was started 2 h after deployment of the flow chamber; thus, it took more than 8 h to collect four samples. In addition to the gas samples emitted from the soil, ambient air in the forest was sampled into two 3-L vacuum stainless steel canisters (SilcoCan, Restek).

### 2.3 Sampling and analysis of forested soil

After collecting the gas samples to determine  $\text{N}_2\text{O}$ , a soil sample (approximately 150 g) was randomly collected from more than four places beneath the chamber.

Approximately 20 g of the soil sample was heated at 80 °C for 48 h to estimate the water content from the weight loss and water-filled pore space (WFPS; the calculation was detailed in Text S1). Using the remaining soil sample (120 g),  $\text{NH}_4^+$ ,  $\text{NO}_3^-$ , and  $\text{NO}_2^-$  in each soil sample were extracted into 120 mL of a 2-M KCl solution, and their concentrations were determined using a high performance microflow analyzer (QuAAtro 39 Autoanalyzer, BLTEC, Osaka, Japan).

## 2.4 Concentration and isotopic compositions of $\text{N}_2\text{O}$

The gas samples collected in aluminum bags or stainless canisters were subsampled into a 100-ml pre-evacuated glass bottle to determine the concentration ( $[\text{N}_2\text{O}]$ ),  $\delta^{15}\text{N}$ , and  $\delta^{18}\text{O}$  of  $\text{N}_2\text{O}$  simultaneously. The remaining samples were further subsampled to either 1 or 2 L pre-evacuated glass bottles to determine the  $\Delta^{17}\text{O}$  of  $\text{N}_2\text{O}$ . The concentration and isotopic compositions ( $\delta^{15}\text{N}$ ,  $\delta^{18}\text{O}$ , and  $\Delta^{17}\text{O}$ ) of  $\text{N}_2\text{O}$  were determined using a continuous flow isotope ratio mass spectrometry (CF-IRMS; Finnigan MAT252, Thermo Fisher Scientific, Waltham, MA, USA) system that consists of an original pre-concentrator system, chemical traps, and gas chromatograph at Nagoya University (Komatsu et al., 2008). The analytical procedures using the CF-IRMS system were the same as those detailed in previous studies (Hirota et al., 2010; Komatsu et al., 2008).

The isotopic ratios of  $^{15}\text{N}/^{14}\text{N}$ ,  $^{17}\text{O}/^{16}\text{O}$ , and  $^{18}\text{O}/^{16}\text{O}$  are expressed in the  $\delta$  notations:

$$\delta^{15}\text{N}, \delta^{17}\text{O}, \text{ or } \delta^{18}\text{O} = R_{\text{sample}}/R_{\text{standard}} - 1 \quad (1)$$

where R denotes  $^{15}\text{N}/^{14}\text{N}$ ,  $^{17}\text{O}/^{16}\text{O}$ , or  $^{18}\text{O}/^{16}\text{O}$  ratios of the sample and each standard reference material.



The  $\Delta^{17}\text{O}$  of  $\text{N}_2\text{O}$ , including  $\text{NO}_2^-$ ,  $\text{NO}_3^-$ ,  $\text{H}_2\text{O}$ , and  $\text{O}_2$ , is defined by Eq. 2 (Kaiser et al., 2007; Miller, 2002):

$$\Delta^{17}\text{O} = \frac{1 + \delta^{17}\text{O}}{(1 + \delta^{18}\text{O})^\beta} - 1 \quad (2)$$

where  $\beta$  denotes the slope of the reference line in the  $\delta^{17}\text{O}$ – $\delta^{18}\text{O}$  space. Previous studies have proposed values ranging from 0.525 to 0.5305 for  $\beta$  during the various processes of isotope fractionation through experimental measurements and/or theoretical calculations (Cao and Liu, 2011; Matsuhisa et al., 1978; Pack and Herwartz, 2014; Sharp and Wostbrock, 2021). In this study, we adopted a value of 0.528 for  $\beta$  to define  $\Delta^{17}\text{O}$ . The details of the ranges of the possible  $\Delta^{17}\text{O}$  variations due to the ranges of  $\beta$  are presented in Section 4.1.

To calibrate the  $\delta^{15}\text{N}$  and  $\delta^{18}\text{O}$  of  $\text{N}_2\text{O}$  to the international scale,  $\text{N}_2\text{O}$  in a tropospheric air sample collected at Hateruma Island in 2010 (Japan) was used as the standard with a  $\delta^{15}\text{N}$  value of +6.5 ‰ and a  $\delta^{18}\text{O}$  value of +44.3 ‰ (Toyoda et al., 2013). To calibrate the  $\Delta^{17}\text{O}$  of  $\text{N}_2\text{O}$  on the international VSMOW (Vienna Standard Mean Ocean Water) scale, we prepared two kinds of  $\text{N}_2\text{O}$  standards with different  $\Delta^{17}\text{O}$  values calibrated using a conventional method (Thiemens and Trogler, 1991). The procedures for this calibration are presented in Section 2.6, with the details of the  $\text{N}_2\text{O}$  standards. Through repeated measurements of  $\text{N}_2\text{O}$  in a tropospheric air sample collected at Nagoya University, the analytical precisions ( $1\sigma$ ) of the measurements were estimated to be  $\pm 10.0$  ppb,  $\pm 0.5$  ‰,  $\pm 0.6$  ‰, and  $\pm 0.11$  ‰ for concentration,  $\delta^{15}\text{N}$ ,  $\delta^{18}\text{O}$ , and  $\Delta^{17}\text{O}$ , respectively (Figure S2). To achieve higher precision, analyses of  $\Delta^{17}\text{O}$  were performed at least three times for each sample, resulting in a standard error (SE) of  $\pm 0.06$  ‰.

## 2.5 Emission flux

Based on the change in the concentration of N<sub>2</sub>O from the inlet to the outlet, the emission flux of N<sub>2</sub>O from the soil was calculated using Eq. 3:

$$\text{Flux} = \frac{P \times V \times (C_{\text{final}} - C_{\text{air}}) \times M}{R \times T \times t \times A} \quad (3)$$

where Flux denotes the emission flux of N<sub>2</sub>O (μg N m<sup>-2</sup> h<sup>-1</sup>), P denotes the pressure (Pa), V represents the volume of the gas sample in the aluminum bag (0.0045 m<sup>3</sup>), C<sub>final</sub> denotes the concentration of N<sub>2</sub>O in the gas sample taken at the end of each deployment of the chamber (μmol mol<sup>-1</sup>), C<sub>air</sub> denotes the concentration of N<sub>2</sub>O in the ambient air (μmol mol<sup>-1</sup>), M represents the molecular weight of N in N<sub>2</sub>O (28 μg N μmol<sup>-1</sup>), R represents the universal gas constant (8.314 m<sup>3</sup> Pa K<sup>-1</sup> mol<sup>-1</sup>), T represents the air temperature in the forest (K), t represents the duration of each gas sampling (45 min), and A represents the surface area of soil covered by the chamber (0.24 m<sup>2</sup>).

## 2.6 Calibration of the Δ<sup>17</sup>O values of N<sub>2</sub>O

To determine the Δ<sup>17</sup>O values of N<sub>2</sub>O in the samples on the VSMOW scale, we prepared two standards (STD1 and STD2) containing N<sub>2</sub>O. The Δ<sup>17</sup>O values of N<sub>2</sub>O in the standards were calibrated to the VSMOW scale using the conventional method reported in (Thiemens and Trogler, 1991), where N<sub>2</sub>O was quantitatively converted to O<sub>2</sub> using BrF<sub>5</sub> and a Ni catalytic container. The details are presented below.

A calibrated quantity of N<sub>2</sub>O (50–170 μmol) was subsampled and transferred into a nickel tube (approximately 60 cm<sup>3</sup>) under liquid N<sub>2</sub> temperature. The coexisting components of N<sub>2</sub>O, such as helium in the case of STD2, were evacuated from the nickel tube after N<sub>2</sub>O was trapped in the nickel tube under liquid N<sub>2</sub> temperature. The nickel

217 tube was then heated at 725 °C for 2.5 h to convert N<sub>2</sub>O to NiO and N<sub>2</sub>. After evacuating  
218 N<sub>2</sub> from the nickel tube, a 10-fold quantity of BrF<sub>5</sub> was introduced into the nickel tube  
219 and heated at 725 °C for 12 h to convert NiO to O<sub>2</sub> and NiF<sub>2</sub>. After the purification of O<sub>2</sub>,  
220 both  $\delta^{18}\text{O}$  and  $\Delta^{17}\text{O}$  of O<sub>2</sub> were determined on the VSMOW scale using IRMS, with the  
221 quantity of O<sub>2</sub> evolved from N<sub>2</sub>O. Details on the procedures of O<sub>2</sub> purification and the  
222 measurement of O<sub>2</sub> using IRMS on the VSMOW scale have been described in previous  
223 studies (Sambuichi et al., 2021, 2023). STD1 is pure N<sub>2</sub>O gas prepared from N<sub>2</sub>O in a gas  
224 cylinder (more than 99.9 %; Koike Medical Ltd., Japan). The yield ratio of O<sub>2</sub> and  $\Delta^{17}\text{O}$   
225 of STD1 were  $103 \pm 7$  % and  $-0.22 \pm 0.07$  ‰, respectively (Figure S3). The N<sub>2</sub>O in STD2  
226 is a mixture of helium and N<sub>2</sub>O (N<sub>2</sub>O/He  $\approx 1.5$ ) produced from NO<sub>2</sub><sup>-</sup> that had been under  
227 oxygen isotope exchange equilibrium with H<sub>2</sub>O with a  $\Delta^{17}\text{O}$  value of +1.2 ‰ originally,  
228 under a pH of 1.2. NO<sub>2</sub><sup>-</sup> was then converted to N<sub>2</sub>O through a reaction with hydrazoic  
229 acid (N<sub>3</sub>H), as described by (Tsunogai et al., 2008). The reaction product (N<sub>2</sub>O) was  
230 purged from the vial using pure helium (more than 99.9 %). After the removal of H<sub>2</sub>O by  
231 passing a trap under the temperature of dry ice + ethanol, N<sub>2</sub>O was captured in a trap at  
232 the temperature of liquid O<sub>2</sub> and then transported into a 1-L stainless steel canister  
233 together with helium. The yield of O<sub>2</sub> and  $\Delta^{17}\text{O}$  of STD2 were  $97 \pm 5$  % and  
234  $+1.13 \pm 0.02$  ‰, respectively (Figure S3). To calibrate the  $\Delta^{17}\text{O}$  values of the samples  
235 measured using CF-IRMS, approximately 1 mL of each STD was subsampled into a 200-  
236 mL pre-evacuated glass bottle and diluted using pure helium to 1 atm. The  $\Delta^{17}\text{O}$  values of  
237 N<sub>2</sub>O in the diluted standards were then determined using CF-IRMS like the procedure  
238 used on the samples before the sample measurements by introducing 30–60 nmol of N<sub>2</sub>O.

This allowed us to calibrate the  $\Delta^{17}\text{O}$  values of the samples to the VSMOW scale (Figure S4).

## 2.7 Isotopic composition of $\text{NO}_2^-$

To determine the  $\delta^{18}\text{O}$  and  $\Delta^{17}\text{O}$  values of soil  $\text{NO}_2^-$  that had been extracted in the KCl solution, the  $\text{NO}_2^-$  in the KCl solution was chemically converted to  $\text{N}_2\text{O}$  using the method originally developed to determine the  $\delta^{18}\text{O}$  of  $\text{NO}_2^-$  (McIlvin and Altabet, 2005), with several modifications for  $\Delta^{17}\text{O}$  (Xu et al., 2021), as explained below. Approximately 40 mL of each solution was pipetted into a glass vial (66.7 mL) and sealed with a butyl rubber septum cap. After purging the solution using high-purity helium for 45 min, 1.8 mL of an azide-acetic acid buffer ( $0.1 \text{ mol L}^{-1} \text{ NaN}_3$  in 1 vol. % acetic acid), which had been purged using pure helium as well, was added to the solution to convert  $\text{NO}_2^-$  to  $\text{N}_2\text{O}$ :



After the vials were shaken for 1 h at a rate of  $2 \text{ cycles s}^{-1}$ , 0.9 mL of 6-M NaOH was added to each vial and shaken for 15 min.

The  $\delta^{18}\text{O}$  and  $\Delta^{17}\text{O}$  of  $\text{N}_2\text{O}$  converted from  $\text{NO}_2^-$  in each vial were determined using the CF-IRMS system. We repeated the analyses for each solution sample at least three times to obtain better precision for  $\Delta^{17}\text{O}$ .

The  $\delta^{18}\text{O}$  values of  $\text{NO}_2^-$  were calibrated to the VSMOW scale using three in-house nitrite standards (STD10, STD11, and STD12), the  $\delta^{18}\text{O}$  values of which had been determined using a thermal conversion/elemental analyzer IRMS system, where oxygen atoms in each nitrite/nitrate had been converted into CO using a glassy carbon tube at

1400 °C (Xu et al., 2021) and calibrated to the VSMOW scale using the international nitrate standards USGS34 ( $\delta^{18}\text{O} = -27.9\text{‰}$ ) and IAEA-NO-3 ( $\delta^{18}\text{O} = +25.6\text{‰}$ ) as the primary standards. Isotope fractionations during chemical conversion into  $\text{N}_2\text{O}$  were corrected by measuring the nitrite standards in the same way as samples were measured using the CF-IRMS system. In addition, the extent of oxygen isotope exchange between  $\text{NO}_2^-$  and  $\text{H}_2\text{O}$  during the conversion was quantified using the relation between  $\delta^{18}\text{O}$  of the nitrite standards and that of  $\text{N}_2\text{O}$  (Xu et al., 2021). The  $\Delta^{17}\text{O}$  values of  $\text{NO}_2^-$  were calibrated to the VSMOW scale by comparing  $\text{N}_2\text{O}$  derived from  $\text{NO}_2^-$  with  $\text{N}_2\text{O}$  standards (STD1 and STD2) while assuming that the changes in  $\Delta^{17}\text{O}$  were negligible during the conversion from  $\text{NO}_2^-$  into  $\text{N}_2\text{O}$ , except for the oxygen isotope exchange reaction between  $\text{NO}_2^-$  and  $\text{H}_2\text{O}$  during the conversion to  $\text{N}_2\text{O}$ . The progress of oxygen isotope exchange between  $\text{NO}_2^-$  and  $\text{H}_2\text{O}$  was calibrated from the  $\Delta^{17}\text{O}$  values of  $\text{NO}_2^-$  using the exchange rate estimated by calculating  $\delta^{18}\text{O}$  values while assuming that the  $\Delta^{17}\text{O}$  value of  $\text{H}_2\text{O}$  was 0 ‰.

While the KCl solutions were widely used for the extraction of soil  $\text{NO}_2^-$  (e.g., Lewicka-Szczebak et al., 2021; Shen et al., 2003), Homyak et al. (2015) raised the concerns that the recovery of soil  $\text{NO}_2^-$  could be low when using KCl solutions compared to deionized water. Therefore, we conducted a comparative experiment to evaluate this potential issue and concluded that the use of KCl solution introduced negligible bias in terms of soil  $\text{NO}_2^-$  recovery or  $\Delta^{17}\text{O}$  measurements compared to deionized water extraction for the soil type and experimental conditions in this study. The details are described in the supplement (Text S2).

### 3. Results

#### 3.1 Flux and isotopic compositions of N<sub>2</sub>O emitted from forested soil

Almost all of the concentrations of N<sub>2</sub>O ([N<sub>2</sub>O]) in the samples collected in aluminum bags were higher than that of N<sub>2</sub>O in ambient air (Figures 3a and S5), implying that N<sub>2</sub>O in the aluminum bags was a mixture of N<sub>2</sub>O in ambient air and N<sub>2</sub>O emitted from the forested soil. To determine the isotopic compositions ( $\delta^{15}\text{N}$ ,  $\delta^{18}\text{O}$ , and  $\Delta^{17}\text{O}$ ) of N<sub>2</sub>O emitted from the soil, N<sub>2</sub>O derived from ambient air was excluded using the linear correlation between 1/[N<sub>2</sub>O] and the isotopic compositions ( $\delta^{15}\text{N}$ ,  $\delta^{18}\text{O}$ , and  $\Delta^{17}\text{O}$ ) during mixing (Figures 3b, 3c, 3d, and S5), also was known as Keeling plot approach (Keeling, 1958; Tsunogai et al., 1998, 2003). This method assumes that the concentrations of N<sub>2</sub>O (N<sub>2</sub>O/(N<sub>2</sub>O + N<sub>2</sub>)) in the gases emitted from the soil were more than 3 %, allowing 1/[N<sub>2</sub>O] to be approximated to be 0 (Text S3). The uncertainties associated with the isotopic compositions of N<sub>2</sub>O emitted from soil (i.e., the intercept) were estimated by applying the York method (Tsunogai et al., 2011; York et al., 2004) to the obtained relationship between 1/[N<sub>2</sub>O] as the independent variable and the isotopic compositions as the dependent variable in which uncertainties of both independent and dependent variables for individual data are considered.

The flux of N<sub>2</sub>O emitted from the forested soil determined on fine days varied from -0.2 to 9.8  $\mu\text{g N m}^{-2} \text{h}^{-1}$ , with an average of  $3.8 \pm 3.1 \mu\text{g N m}^{-2} \text{h}^{-1}$  (1SD; n = 12). In addition, the emission flux during the warm seasons (from April to October;  $5.1 \pm 2.8 \mu\text{g N m}^{-2} \text{h}^{-1}$ ) was significantly higher than that during the cold seasons (from November to March;  $1.0 \pm 1.1 \mu\text{g N m}^{-2} \text{h}^{-1}$ ) (Figure 4a; Table S1), implying that the emission flux of

N<sub>2</sub>O on fine days exhibited clear seasonal variation. Furthermore, the average emission flux of N<sub>2</sub>O determined on rainy days ( $38.8 \pm 28.0 \mu\text{g N m}^{-2} \text{h}^{-1}$ ;  $n = 6$ ) was significantly higher than that determined on fine days ( $3.8 \pm 3.1 \mu\text{g N m}^{-2} \text{h}^{-1}$ ) (Figures 4a and 4b). These patterns of N<sub>2</sub>O emissions were in accordance with those of agricultural and forested soils reported in previous studies (Anthony et al., 2023; Chen et al., 2012; Choudhary et al., 2002; Yan et al., 2008).

Because of the small emission flux of N<sub>2</sub>O during the cold seasons, the linear relationships between the isotopic compositions and  $1/[\text{N}_2\text{O}]$  became insignificant in some of the observations performed during the cold seasons (Figure S5, from Nov. 2022 to Jan. 2023). Thus, the uncertainties associated with the isotopic compositions estimated for N<sub>2</sub>O emitted from the soil became enormous. Consequently, the isotopic compositions of N<sub>2</sub>O emitted from the soil are not shown under the following conditions: (1) the  $[\text{N}_2\text{O}]$  in the gas sample collected at the end of each deployment of the chamber did not exceed 130 % of that of ambient air, and (2) the linear correlation between  $1/[\text{N}_2\text{O}]$  and the isotopic compositions was statistically insignificant ( $P > 0.05$ ). Similar criteria have been adopted in previous studies (Kaushal et al., 2022; Opdyke et al., 2009).

The N<sub>2</sub>O emitted from the forested soil on fine days exhibited  $\delta^{15}\text{N}$ ,  $\delta^{18}\text{O}$ , and  $\Delta^{17}\text{O}$  values ranging from  $-27.5 \text{ ‰}$  to  $-17.9 \text{ ‰}$ , from  $+26.1 \text{ ‰}$  to  $+37.6 \text{ ‰}$ , and from  $-0.40 \text{ ‰}$  to  $-0.11 \text{ ‰}$ , respectively, with average values and standard deviations (1SD) of  $-22.5 \pm 2.8 \text{ ‰}$ ,  $+30.9 \pm 4.3 \text{ ‰}$ , and  $-0.30 \pm 0.09 \text{ ‰}$ , respectively (Figures 4g, 4e, and 4c). On the other hand, N<sub>2</sub>O emitted from the forested soil on rainy days exhibited  $\delta^{15}\text{N}$ ,  $\delta^{18}\text{O}$ , and  $\Delta^{17}\text{O}$  values ranging from  $-26.6 \text{ ‰}$  to  $-13.8 \text{ ‰}$ , from  $+18.4 \text{ ‰}$  to  $+36.2 \text{ ‰}$ , and from

–0.06 ‰ to +0.26 ‰, respectively, with average values and standard deviations (1SD) of –20.4±5.0 ‰, +27.9±6.4 ‰, and +0.12±0.13 ‰, respectively (Figures 4g, 4e, and 4c).

The NO<sub>2</sub><sup>–</sup> exhibited δ<sup>18</sup>O and Δ<sup>17</sup>O values ranging from +2.4 ‰ to +12.0 ‰ and from +0.04 to +0.50 ‰, respectively, with average values of +6.0±2.0 ‰ and +0.23±0.12 ‰, respectively (n = 18, Figures 4e and 4c). These δ<sup>18</sup>O values of NO<sub>2</sub><sup>–</sup> coincided well with those determined in a previous study (Lewicka-Szczebak et al., 2021).

### 3.2 Flux and isotopic compositions of N<sub>2</sub>O emitted from artificially fertilized soils

The fluxes of N<sub>2</sub>O emitted from the NF (no fertilizer), U (fertilized with urea, CO(NH<sub>2</sub>)<sub>2</sub>), and CS (fertilized with Chile saltpeter, KNO<sub>3</sub>) plots were 5.2, 70.6, and 112.3 μg N m<sup>–2</sup> h<sup>–1</sup>, respectively, 2 days after fertilization and 4.2, 56.7, and 39.4 μg N m<sup>–2</sup> h<sup>–1</sup>, respectively, 6 days after fertilization (Table S1). The fluxes of N<sub>2</sub>O emitted from the U and CS plots were significantly higher than that from the NF plot, indicating that the flux of N<sub>2</sub>O emitted from the soil increased significantly because of fertilization, supporting the results reported in previous studies (Kaushal et al., 2022; McKenney et al., 1978; Toyoda et al., 2011, 2017).

The δ<sup>15</sup>N, δ<sup>18</sup>O, and Δ<sup>17</sup>O values of N<sub>2</sub>O emitted from the NF plot 2 days after fertilization were –17.1±6.4 ‰, +36.1±6.7 ‰, and –0.37±0.20 ‰, respectively, whereas those emitted from the NF plot 6 days after fertilization were –12.2±3.2 ‰, +40.0±13.3 ‰, and –0.32±0.23 ‰, respectively. The δ<sup>15</sup>N, δ<sup>18</sup>O, and Δ<sup>17</sup>O values of N<sub>2</sub>O emitted from the U plot 2 days after fertilization were –39.3±0.7 ‰, +34.4±0.4 ‰, and –0.14±0.06 ‰, respectively, whereas those emitted from the U plot 6 days after fertilization were –33.3±0.5 ‰, +25.7±0.6 ‰, and –0.16±0.05 ‰, respectively. The



$\delta^{15}\text{N}$ ,  $\delta^{18}\text{O}$ , and  $\Delta^{17}\text{O}$  values of  $\text{N}_2\text{O}$  emitted from the CS plot 2 days after fertilization were  $-19.3 \pm 0.6$  ‰,  $+54.1 \pm 0.8$  ‰, and  $+8.22 \pm 0.03$  ‰, respectively, whereas those emitted from the CS plot 6 days after fertilization were  $-11.3 \pm 0.7$  ‰,  $+58.7 \pm 1.2$  ‰, and  $+7.36 \pm 0.17$  ‰, respectively (Figure 5). These flux,  $\delta^{15}\text{N}$ , and  $\delta^{18}\text{O}$  of  $\text{N}_2\text{O}$  emitted from the NF, U, and CS plots correspond well with the results of many previous studies on forested and artificial soils (or agricultural soils) (Kaushal et al., 2022; Kim and Craig, 1993; Snider et al., 2009; Toyoda et al., 2017; Wrage et al., 2004).

The  $\delta^{18}\text{O}$  and  $\Delta^{17}\text{O}$  values of  $\text{NO}_2^-$  in the NF plot 2 days after fertilization were  $+2.7$  ‰ and  $+0.42$  ‰, respectively, whereas those in the NF plot 6 days after fertilization were  $+1.3$  ‰ and  $+0.35$  ‰, respectively. The  $\delta^{18}\text{O}$  and  $\Delta^{17}\text{O}$  values of  $\text{NO}_2^-$  in the U plot 2 days after fertilization were  $+7.6$  ‰ and  $+0.31$  ‰, respectively, whereas those in the U plot 6 days after fertilization were  $+5.4$  ‰ and  $+0.17$  ‰, respectively. The  $\delta^{18}\text{O}$  and  $\Delta^{17}\text{O}$  values of  $\text{NO}_2^-$  in the CS plot 2 days after fertilization were  $+29.0$  ‰ and  $+8.26$  ‰, respectively, whereas those in the CS plot 6 days after fertilization were  $+45.2$  ‰ and  $+12.32$  ‰, respectively (Figure 6).

## 4. Discussion

### 4.1 Identification of $\text{N}_2\text{O}$ production pathways in forested soil using $\Delta^{17}\text{O}$ signature

Because O atoms in  $\text{N}_2\text{O}$  emitted from soil can be derived from those in  $\text{NO}_2^-$ ,  $\text{O}_2$ , or  $\text{H}_2\text{O}$  in soil (Figure 1), we can constrain the pathways of  $\text{N}_2\text{O}$  production by comparing the  $\delta^{18}\text{O}$  and  $\Delta^{17}\text{O}$  values of  $\text{N}_2\text{O}$  with those of  $\text{NO}_2^-$ ,  $\text{O}_2$ , and  $\text{H}_2\text{O}$  in soil. Consequently, we compiled the  $\delta^{18}\text{O}$  and  $\Delta^{17}\text{O}$  values of atmospheric  $\text{O}_2$  ( $+23.88$  ‰ for  $\delta^{18}\text{O}$  and  $-0.44$  ‰ for  $\Delta^{17}\text{O}$ , (Sharp and Wostbrock, 2021)) and rainwater (ranging from  $-2$  ‰ to

375  $-10\text{ ‰}$  for  $\delta^{18}\text{O}$  in Japan, (Nakagawa et al., 2018; Takahashi, 1998; Uechi and Uemura,  
376 2019; Zou et al., 2015);  $+0.03\text{ ‰}$  for  $\Delta^{17}\text{O}$  in Japan (Uechi and Uemura, 2019)), as  
377 shown in Figures 4 and 6, along with those of soil  $\text{NO}_2^-$  measured in this study.

378 The  $\Delta^{17}\text{O}$  of  $\text{N}_2\text{O}$  produced in the soil may differ from that of the source of O atoms  
379 ( $\text{O}_2$ ,  $\text{NO}_2^-$ ,  $\text{H}_2\text{O}$ ) because of oxygen isotope fractionation during nitrification and  
380 denitrification, as the value of  $\beta$  in Eq. (2) may vary depending on the reactions. Thus,  
381 prior to using  $\Delta^{17}\text{O}$  values to identify the pathways of  $\text{N}_2\text{O}$  production in soils, we  
382 quantified the possible variations in the  $\Delta^{17}\text{O}$  values of  $\text{N}_2\text{O}$  during each reaction. The  
383 details are presented below.

384 The fractionation of oxygen isotopes during the transformation of the O atoms in  $\text{O}_2$  to  
385 those in  $\text{N}_2\text{O}$  through nitrification accompanies significant variations in the value of  $\delta^{18}\text{O}$   
386 from  $\text{O}_2$  to  $\text{N}_2\text{O}$  (Figures 4e and 6a). In addition to  $\delta^{18}\text{O}$ , the  $\Delta^{17}\text{O}$  value of  $\text{N}_2\text{O}$  produced  
387 through nitrification could be somewhat different from that of  $\text{O}_2$ , even if all O atoms in  
388  $\text{N}_2\text{O}$  were derived from  $\text{O}_2$ , due to the possible differences in  $\beta$  from 0.528 during the  
389 reaction (Figure 7). The average variation in  $\delta^{18}\text{O}$  from  $\text{O}_2$  to  $\text{N}_2\text{O}$  due to nitrification  
390 ( $\Delta\delta^{18}\text{O}(\text{N}_2\text{O}-\text{O}_2)$ ) was estimated to be  $9\text{ ‰}$  on average (Figures 4e and 6a) based on the  
391 difference in  $\delta^{18}\text{O}$  values between  $\text{N}_2\text{O}$  emitted from the soil in this study ( $+33\pm 10\text{ ‰}$ ;  $n$   
392  $= 19$ ) and  $\text{O}_2$  in the literature (Sharp and Wostbrock, 2021). Conversely, we can expect  
393 values from 0.525 to 0.5305 for  $\beta$  in the various reactions (Cao and Liu, 2011; Matsuhisa  
394 et al., 1978; Pack and Herwartz, 2014; Sharp and Wostbrock, 2021), where the  $\beta$  of  
395 nitrification may be included. Thus, we quantified the possible range of variations in the  
396  $\Delta^{17}\text{O}$  value of  $\text{N}_2\text{O}$  from that of  $\text{O}_2$  to be less than  $0.027\text{ ‰}$  (Figure 7), based on the  
397 observed  $\Delta\delta^{18}\text{O}(\text{N}_2\text{O}-\text{O}_2)$  and the possible variation range of  $\beta$ .

Similarly, the fractionation of oxygen isotopes during the transformation of O atoms in  $\text{NO}_2^-$  to those in  $\text{N}_2\text{O}$  through denitrification accompanies significant variations in  $\delta^{18}\text{O}$  from  $\text{NO}_2^-$  to  $\text{N}_2\text{O}$  as well. The  $\Delta^{17}\text{O}$  value of  $\text{N}_2\text{O}$  produced through  $\text{NO}_2^-$  reduction could be somewhat different from that of  $\text{NO}_2^-$ , even if all O atoms in  $\text{N}_2\text{O}$  were derived from  $\text{NO}_2^-$ , due to the possible differences in  $\beta$  from 0.528 during the reaction (Figure 7). The average variation in  $\delta^{18}\text{O}$  from  $\text{NO}_2^-$  to  $\text{N}_2\text{O}$  due to fractionation ( $\Delta\delta^{18}\text{O}$  ( $\text{N}_2\text{O}-\text{NO}_2^-$ )) was estimated to be 25 ‰ on average (Figures 4e and 6a) based on the difference in  $\delta^{18}\text{O}$  values between  $\text{N}_2\text{O}$  ( $+33\pm 10$  ‰;  $n = 19$ ) and  $\text{NO}_2^-$  in this study ( $+8\pm 9$  ‰;  $n = 24$ ). Thus, we quantified the possible range of variations in the  $\Delta^{17}\text{O}$  value of  $\text{N}_2\text{O}$  from that of  $\text{NO}_2^-$  to be less than 0.075 ‰ (Figure 7), based on the observed  $\Delta\delta^{18}\text{O}$  ( $\text{N}_2\text{O}-\text{NO}_2^-$ ) and the possible variation range of  $\beta$ , from 0.525 to 0.5305.

Similarly, kinetic fractionation during the reduction of  $\text{N}_2\text{O}$  to  $\text{N}_2$  accompanies variation in  $\delta^{18}\text{O}$  from original  $\text{N}_2\text{O}$  to residual  $\text{N}_2\text{O}$  as well. The  $\Delta^{17}\text{O}$  value of residual  $\text{N}_2\text{O}$  could somewhat differ from that of the original  $\text{N}_2\text{O}$ . Previous studies have reported the range of variations in  $\delta^{18}\text{O}$  from original  $\text{N}_2\text{O}$  to residual  $\text{N}_2\text{O}$  due to kinetic fractionation to be less than 10 ‰ on average through incubation experiments (Lewicka-Szczebak et al., 2014, 2015). Thus, we quantified the possible range of variations in the  $\Delta^{17}\text{O}$  value of residual  $\text{N}_2\text{O}$  from that of original  $\text{N}_2\text{O}$  to be less than 0.03 ‰ (Figure 7), based on  $\Delta\delta^{18}\text{O}$  (less than 10 ‰) and the variation range of  $\beta$ , from 0.525 to 0.5305.

These possible variations in  $\Delta^{17}\text{O}$  (less than 0.075 ‰) were much less than the difference in  $\Delta^{17}\text{O}$  values between  $\text{O}_2$  and  $\text{NO}_2^-$  in the forested soil (0.7 ‰ on average; Figures 4c). In addition, the possible variation ranges in  $\Delta^{17}\text{O}$  become much smaller if the differences in  $\beta$  from 0.528 were smaller than those used in the calculations (from 0.525

to 0.5305). Thus, we concluded that the possible variations in the  $\Delta^{17}\text{O}$  value of  $\text{N}_2\text{O}$  from that of the source molecules of O atoms ( $\text{O}_2$ ,  $\text{H}_2\text{O}$ , and  $\text{NO}_2^-$ ) during the transformations, including nitrification, denitrification, and reduction, were negligible.

While the  $\Delta^{17}\text{O}$  values of soil  $\text{O}_2$  and  $\text{H}_2\text{O}$  used in this study were referred from atmospheric  $\text{O}_2$  and rainwater, respectively, the processes in soil, including diffusion and respiration of  $\text{O}_2$  and evaporation and infiltration of rainwater, may cause significant isotopic fractionations of  $\delta^{18}\text{O}$ , which could consequently alter the  $\Delta^{17}\text{O}$  values of atmospheric  $\text{O}_2$  and rainwater. Thus, prior to using  $\Delta^{17}\text{O}$  values to identify the pathways of  $\text{N}_2\text{O}$  production in soils, we evaluated the possible variations in the  $\Delta^{17}\text{O}$  values of  $\text{O}_2$  and  $\text{H}_2\text{O}$  in soil compared to those of atmospheric  $\text{O}_2$  and rainwater. The details are presented below.

For soil  $\text{O}_2$ , Aggarwal and Dillon (1998) measured the  $\delta^{18}\text{O}$  values in soil gas at a depth of 3-4 m at a site near Lincoln, Nebraska, USA ranged from +23.3 ‰ to +27.2 ‰, showing the values were comparable with that of atmospheric  $\text{O}_2$  (+23.5 ‰ after adjustment in Aggarwal and Dillon. 1998). This confirms that the isotopic fractionations of soil  $\text{O}_2$  induced from soil respiration and diffusion processes weren't significant. Because the maximum variation in  $\delta^{18}\text{O}$  from atmospheric  $\text{O}_2$  to soil  $\text{O}_2$  was less than 3.7 ‰ (27.2 ‰ – 23.5 ‰), using the method presented in Figure 7, we quantified the possible variations in the  $\Delta^{17}\text{O}$  value of soil  $\text{O}_2$  from that of atmospheric  $\text{O}_2$  to be less than 0.01 ‰. Thus, we ignored the negligible variations in this study.

Similarly, for soil  $\text{H}_2\text{O}$ , Lyu (2021) observed that  $\delta^{18}\text{O}$  values in soil  $\text{H}_2\text{O}$  at the depths of 0-5 cm, 15-20 cm, and 40-45 cm in a subtropical forest plantation ranged from –4 ‰ to –10 ‰, which fully overlapped with local rainwater (–1 ‰ to –16 ‰), indicating

insignificant isotopic fractionations of soil H<sub>2</sub>O during hydrological processes such as infiltration and evaporation. Besides, Aron et al. (2021) compiled  $\Delta^{17}\text{O}$  values of terrestrial H<sub>2</sub>O including rainwater, surface and subsurface water in earth, ranged from +0.06 to -0.06 ‰ and didn't show significant difference with each other, which also indicating that the possible variations of  $\Delta^{17}\text{O}$  values of soil H<sub>2</sub>O compared to that of rainwater should be negligible. Finally, we added the variations of  $\Delta^{17}\text{O}$  values (+0.06 to -0.06 ‰) of terrestrial H<sub>2</sub>O reported in Aron et al. (2021) to Figures 4 and 6 as the uncertainties of  $\Delta^{17}\text{O}$  values of soil H<sub>2</sub>O.

In the forested soil, N<sub>2</sub>O exhibited  $\Delta^{17}\text{O}$  values ( $-0.30 \pm 0.09$  ‰ on average) that were close to that of O<sub>2</sub> ( $-0.44$  ‰) but deviated from those of soil NO<sub>2</sub><sup>-</sup> on fine days ( $+0.24 \pm 0.14$  ‰; Figures 4c and 4d), implying that nitrification was the main pathway to produce N<sub>2</sub>O in the soil on fine days. Conversely, N<sub>2</sub>O emitted from the soil on rainy days exhibited  $\Delta^{17}\text{O}$  values ( $+0.12 \pm 0.13$  ‰) that were close to those of soil NO<sub>2</sub><sup>-</sup> ( $+0.22 \pm 0.09$  ‰) and soil H<sub>2</sub>O ( $+0.03$  ‰) but deviated from that of O<sub>2</sub> (Figures 4c and 4d), implying that (1) the main pathway to produce N<sub>2</sub>O changed from nitrification on fine days to denitrification on rainy days and/or (2) the possible contribution of O atoms derived from soil H<sub>2</sub>O became more active during the production of N<sub>2</sub>O in the soil on rainy days.

## **4.2 Changes in the $\Delta^{17}\text{O}$ of N<sub>2</sub>O emitted from artificially fertilized soils**

To quantitatively constrain the possible contributions of O atoms derived from soil H<sub>2</sub>O during the production of N<sub>2</sub>O in the soil, we observed changes in the isotopic compositions of N<sub>2</sub>O from the same soil in response to artificial fertilization. In the plot

467 fertilized with CS, the  $\Delta^{17}\text{O}$  value of  $\text{N}_2\text{O}$  emitted from the soil ( $+7.79 \pm 0.61$  ‰ on the  
 468 average of 2 and 6 days after the fertilization) became significantly closer to that of soil  
 469  $\text{NO}_2^-$  ( $+10.3 \pm 2.9$  ‰) compared with that of atmospheric  $\text{O}_2$  ( $-0.44$  ‰; Figure 6b). This  
 470 suggested that denitrification became the main pathway of  $\text{N}_2\text{O}$  production, probably  
 471 because of fertilization, which resulted in a significantly higher concentration of  $\text{NO}_3^-$   
 472 ( $278.4 \pm 43.2$  mg N  $\text{kg}^{-1}$ ; Table S1) than that of  $\text{NH}_4^+$  ( $15.8 \pm 4.1$  mg N  $\text{kg}^{-1}$ ) in the CS plot.  
 473 In addition,  $\text{N}_2\text{O}$  emitted from the CS plot exhibited  $\Delta^{17}\text{O}$  values that were significantly  
 474 different from those of soil  $\text{H}_2\text{O}$  ( $+0.03$  ‰; Figure 6b), implying that the contribution of  
 475 O atoms derived from soil  $\text{H}_2\text{O}$  was minor during the reduction of  $\text{NO}_2^-$  to produce  $\text{N}_2\text{O}$ .  
 476 If all the O atoms with low  $\Delta^{17}\text{O}$  values in  $\text{N}_2\text{O}$  were derived from soil  $\text{H}_2\text{O}$  ( $+0.03$  ‰) in  
 477 the CS plot, the contribution of O atoms derived from soil  $\text{H}_2\text{O}$  was calculated to be 24 %  
 478  $((10.30 \text{ ‰} - 7.79 \text{ ‰}) / (10.30 \text{ ‰} - 0.03 \text{ ‰}))$ , based on the isotopic mass balance. If the  
 479  $\text{O}_2$  also contributed to the  $\text{N}_2\text{O}$  production in the CS plot, the contribution of O atoms  
 480 derived from soil  $\text{H}_2\text{O}$  should be further reduced. As a result, we determined that the  
 481 maximum possible contribution of O atoms derived from soil  $\text{H}_2\text{O}$  during the reduction  
 482 of  $\text{NO}_2^-$  to  $\text{N}_2\text{O}$  was 24 %.

483 On the other hand, in the plot fertilized with urea (U plot), the  $\Delta^{17}\text{O}$  value of  $\text{N}_2\text{O}$   
 484 ( $-0.15 \pm 0.01$  ‰) was close to that of  $\text{O}_2$  ( $-0.44$  ‰) compared with that of soil  $\text{NO}_2^-$   
 485 ( $+0.24 \pm 0.10$  ‰). This suggested that nitrification was the main pathway of  $\text{N}_2\text{O}$   
 486 production (Figure 6b), probably due to the enhancement of  $\text{NH}_4^+$  concentration  
 487 ( $423.1 \pm 18.2$  mg N  $\text{kg}^{-1}$ ; Table S1) compared with that of  $\text{NO}_3^-$  ( $13.0 \pm 10.7$  mg N  $\text{kg}^{-1}$ ) in  
 488 the U plot. In addition,  $\text{N}_2\text{O}$  emitted from the U plot exhibited  $\Delta^{17}\text{O}$  values that were  
 489 significantly different from that of soil  $\text{H}_2\text{O}$  ( $+0.03$  ‰; Figure 6b), implying that the

contribution of O atoms derived from soil H<sub>2</sub>O was also minor during the oxidation of NH<sub>4</sub><sup>+</sup> to produce N<sub>2</sub>O. Consequently, the contribution of O atoms derived from soil H<sub>2</sub>O was minor in the soil during N<sub>2</sub>O production, irrespective of the pathways of N<sub>2</sub>O production being either nitrification or denitrification. In addition, it is difficult to explain the observed increases in the emission flux of N<sub>2</sub>O from the soil on rainy days based only on the active contribution of O atoms derived from soil H<sub>2</sub>O. Consequently, we concluded that N<sub>2</sub>O production through denitrification became active in the soil on rainy days, which resulted in increased N<sub>2</sub>O emission and higher  $\Delta^{17}\text{O}$  values.

#### **4.3 Verification of active N<sub>2</sub>O emission by denitrification on rainy days**

The forested soil exhibited significantly lower WFPS on fine days ( $66.1 \pm 6.2$  %; Table S1) than on rainy days ( $95.6 \pm 19.1$  %), implying that the O<sub>2</sub> concentration in the soil was higher on fine days than on rainy days. Using the isotope tracer enriched in <sup>15</sup>N (<sup>15</sup>NO<sub>3</sub><sup>-</sup> or <sup>15</sup>NH<sub>4</sub><sup>+</sup>), Mathieu et al. 2006 estimated the relative importance of nitrification and denitrification to produce N<sub>2</sub>O in soil. They found that nitrification produced the majority of N<sub>2</sub>O under low WFPS conditions (75 %), whereas denitrification accounted for more than 85 % of N<sub>2</sub>O produced under high WFPS conditions (150 %). Similarly, using natural stable isotopes (SP), Ibraim et al. 2019 reported the primary pathway for N<sub>2</sub>O production in a grassland shifted from nitrification to denitrification as increasing WFPS, when WFPS was below 90 %. Thus, we conclude that the lower WFPS in the soil caused oxic conditions on fine days, resulting in nitrification as the primary pathway for N<sub>2</sub>O production in the soil. Conversely, the higher WFPS caused redox conditions in the soil

on rainy days, resulting in active N<sub>2</sub>O production through denitrification in the soil (Figures 4a and 4b).

During continuous monitoring of the emission flux of N<sub>2</sub>O from an agricultural soil for four years, Anthony et al. 2023 found short-term increases in the emission flux during or immediately after rainfall or irrigation. They referred to this high emission flux as "hot moments" and defined it as exceeding four standard deviations of that of normal periods. They also found significant correlations between the emission flux and WFPS, leading to the conclusion that variations in the concentrations of O<sub>2</sub> in surface soils were responsible for the hot moments of N<sub>2</sub>O emissions. Although the hot moments accounted for 1 % of all measurements, they contributed up to 57 % of the annual emissions, indicating their significance as a source of atmospheric emissions. In this study, the emission flux of N<sub>2</sub>O on rainy days also exceeded four standard deviations of that on fine days (Figures 4a and 4b). The  $\Delta^{17}\text{O}$  evidence of N<sub>2</sub>O found in this study further verified that denitrification was mainly responsible for the enhancement of N<sub>2</sub>O production during the hot moments.

#### **4.4 Changes in the pathway of N<sub>2</sub>O production due to fertilization with urea**

During our observation on the plot fertilized with urea (U plot), N<sub>2</sub>O emitted from the plot exhibited  $\Delta^{17}\text{O}$  values ( $-0.15 \pm 0.01$  ‰ on average; Figure 6b) that were significantly higher than those of the plot without fertilization (NF plot;  $-0.35 \pm 0.04$  ‰ on average). Although an increase in the contribution of O atoms derived from soil H<sub>2</sub>O could be responsible for the  $\Delta^{17}\text{O}$  values in addition to an increase in N<sub>2</sub>O production through nitrification, we concluded that an increase in N<sub>2</sub>O production through NO<sub>2</sub><sup>-</sup> reduction



was responsible for the  $\Delta^{17}\text{O}$  values ( $-0.15 \pm 0.01$  ‰ on average) of  $\text{N}_2\text{O}$  produced in the plot in response to fertilization of urea/ $\text{NH}_4^+$  for the following reasons.

Avrahami et al. 2002 reported that fertilization with urea/ $\text{NH}_4^+$  in soil promoted the oxidation of  $\text{NH}_4^+$  and thus provided electron acceptors for denitrification. That is, the enrichment of nitrate through nitrification also promotes denitrification. Based on the stable isotopes of  $\text{N}_2\text{O}$  ( $\delta^{15}\text{N}$ ,  $\delta^{18}\text{O}$ , and SP), along with in vitro acetylene blockage experiments on agricultural soils fertilized with  $\text{NH}_4^+$ , Zhang et al. 2016 reported that while 50 %–70 % of  $\text{N}_2\text{O}$  was produced through nitrification, nitrifier denitrification ( $\text{NH}_4^+ \rightarrow \text{NO}_2^- \rightarrow \text{N}_2\text{O}$ ) and/or heterotrophic denitrification ( $\text{NH}_4^+ \rightarrow \text{NO}_3^- \rightarrow \text{NO}_2^- \rightarrow \text{N}_2\text{O}$ ) accounted for 30 %–50 % of  $\text{N}_2\text{O}$  production. Similar results have also been reported in previous studies. Although  $\text{N}_2\text{O}$  production through nitrification was simulated by fertilization with urea/ $\text{NH}_4^+$  in various soils, denitrification also accounted for a significant portion of  $\text{N}_2\text{O}$  production (Kaushal et al., 2022; Khalil et al., 2004; Zhu et al., 2013). In addition to nitrifier/heterotrophic denitrification,  $\text{N}_2\text{O}$  produced through the anammox process ( $\text{NH}_4^+ + \text{NO}_2^- \rightarrow \text{N}_2\text{O}$ , Okabe et al., 2011; Tang et al., 2011; Tsushima et al., 2007) can be responsible for the reduction of  $\text{NO}_2^-$  as well. Zhu et al. 2011 found that the highest rate of anammox was comparable with that of denitrification in soils fertilized with  $\text{NH}_4^+$  ( $6.2$ – $178.8$  mg N  $\text{kg}^{-1}$ ). These previous experiments support our observation on the U plot that the addition of urea/ $\text{NH}_4^+$  stimulates  $\text{N}_2\text{O}$  production through nitrifier denitrification and/or heterotrophic denitrification, and/or anammox reaction in addition to nitrification. The increased  $\text{NO}_3^-$  concentration in the U plot ( $13.0 \pm 10.7$  mg N  $\text{kg}^{-1}$ ) compared with those in the NF plot ( $2.3 \pm 0.5$  mg N  $\text{kg}^{-1}$ ) probably

due to nitrification stimulated by the addition of  $\text{NH}_4^+$  may be responsible for the active reduction of  $\text{NO}_2^-$ .

#### **4.5 Stable $\Delta^{17}\text{O}$ as a natural signature for identifying $\text{N}_2\text{O}$ production pathways**

Although the  $\delta^{18}\text{O}$  values of  $\text{N}_2\text{O}$  emitted from the soil were significantly higher than those of the sources of O atoms in  $\text{N}_2\text{O}$  ( $\text{NO}_2^-$ ,  $\text{O}_2$ , and  $\text{H}_2\text{O}$ ; Figures 4e and 6a) due to the fractionations of oxygen isotopes during the production and/or reduction of  $\text{N}_2\text{O}$ , the  $\Delta^{17}\text{O}$  values of  $\text{N}_2\text{O}$  remained within the range of these sources. This indicates that  $\Delta^{17}\text{O}$  primarily reflects the pathways of  $\text{N}_2\text{O}$  production, providing information distinct from the  $\delta^{18}\text{O}$  signature because  $\Delta^{17}\text{O}$  is stable during the processes of biogeochemical isotope fractionation. Moreover, while  $\text{N}_2\text{O}$  emission from the forested soil did not show significant differences in  $\delta^{15}\text{N}$  and  $\delta^{18}\text{O}$  values between fine and rainy days due to the fractionations of nitrogen and oxygen isotopes (Figures 4f and 4h), the significant difference in the  $\Delta^{17}\text{O}$  values of  $\text{N}_2\text{O}$  between fine and rainy days (Figure 4d) highlights  $\Delta^{17}\text{O}$  to be a promising natural signature for identifying the pathways of  $\text{N}_2\text{O}$  production in soils.

In addition to natural soils, the stable  $\Delta^{17}\text{O}$  signature is expected to be useful for identifying the pathways of  $\text{N}_2\text{O}$  production in various ecosystems, such as agricultural soils and aquatic environments, where the isotopic fractionations of nitrogen and oxygen isotopes involving biogeochemical processes are significant as well. However, in order to identify the pathways of  $\text{N}_2\text{O}$  production quantitatively, the uncertainties, including the  $\beta$  values of each reaction during  $\text{N}_2\text{O}$  production and the contributions of O atoms derived

from soil H<sub>2</sub>O during N<sub>2</sub>O production, should be quantified precisely in the future studies.

## 5. Conclusions

Temporal variations in  $\Delta^{17}\text{O}$  of N<sub>2</sub>O emitted from forested soil were determined to identify the main pathway of N<sub>2</sub>O production. Both  $\Delta^{17}\text{O}$  values and fluxes of N<sub>2</sub>O were significantly higher on rainy days compared to fine days. Besides, the  $\Delta^{17}\text{O}$  values of N<sub>2</sub>O emitted on rainy and fine days were close to those of soil NO<sub>2</sub><sup>-</sup> and O<sub>2</sub>, respectively. Because NO<sub>2</sub><sup>-</sup> and O<sub>2</sub> were the source of O-atoms in N<sub>2</sub>O production through denitrification and nitrification, respectively, we concluded that while nitrification dominated N<sub>2</sub>O production on fine days, denitrification became active on rainy days, resulting in the N<sub>2</sub>O flux increasing. In addition, the  $\Delta^{17}\text{O}$  of N<sub>2</sub>O emitted from the same soil fertilized with either Chile saltpeter or urea exhibited values that were significantly different from those of soil H<sub>2</sub>O, implying that the contributions of O atoms derived from soil H<sub>2</sub>O during N<sub>2</sub>O production were minor. Furthermore, while N<sub>2</sub>O emitted from the forested soil did not show significant differences in  $\delta^{15}\text{N}$  and  $\delta^{18}\text{O}$  values between fine and rainy days, the significant difference in the  $\Delta^{17}\text{O}$  values of N<sub>2</sub>O highlights  $\Delta^{17}\text{O}$  to be a promising natural signature for identifying the pathways of N<sub>2</sub>O production in soils, because  $\Delta^{17}\text{O}$  is almost stable during isotope fractionation processes such as N<sub>2</sub>O production and reduction.

*Data availability.* All the primary data are presented in the Supplement.

*Author contributions.* WD, UT, and FN designed the study. WD, TH, WR, MI, HX, and YK performed the field observations. WD, UT, TS and FN determined the concentrations and isotopic compositions of the samples. WD, TS, FN, and UT performed data analysis.

*Competing interests.* The authors declare that they have no conflict of interest.

*Acknowledgments.*

We thank the anonymous referees for their valuable remarks on an earlier version of this paper. We are grateful to the members of the Biogeochemistry Group at Nagoya University for their valuable support throughout this study. This work was supported by a Grant-in-Aid for Scientific Research from the Ministry of Education, Culture, Sports, Science, and Technology of Japan under grant numbers 22H00561, 17H00780, 22K19846, the Grant-in-Aid for Japan Society for the Promotion of Science Fellows under grant number 23KJ1088, the Yanmar Environmental Sustainability Support Association, the River Fund of the River Foundation, Japan, the Reiwa Environmental Foundation, and the National Research Foundation of Korea Grant from the Korean Government (MSIT; the Ministry of Science and ICT, NRF-2021M1A5A1065425, KOPRI-PN24011).

## **Reference**

Aggarwal, P. K. and Dillon, M. A.: Stable Isotope Composition of Molecular Oxygen in Soil Gas and Groundwater: A Potentially Robust Tracer for Diffusion and Oxygen Consumption Processes, *Geochimica et Cosmochimica Acta*, 62, 577–584, [https://doi.org/10.1016/S0016-7037\(97\)00377-3](https://doi.org/10.1016/S0016-7037(97)00377-3), 1998.

625 Anthony, T. L., Szutu, D. J., Verfaillie, J. G., Baldocchi, D. D., and Silver, W. L.:  
 626 Carbon-sink potential of continuous alfalfa agriculture lowered by short-term nitrous  
 627 oxide emission events, *Nature Communications*, 14, 1926,  
 628 <https://doi.org/10.1038/s41467-023-37391-2>, 2023.

629 Aron, P. G., Levin, N. E., Beverly, E. J., Huth, T. E., Passey, B. H., Pelletier, E. M.,  
 630 Poulsen, C. J., Winkelstern, I. Z., and Yarian, D. A.: Triple oxygen isotopes in the water  
 631 cycle, *Chemical Geology*, 565, 120026, <https://doi.org/10.1016/j.chemgeo.2020.120026>,  
 632 2021.

633 Avrahami, S., Conrad, R., and Braker, G.: Effect of Soil Ammonium Concentration on  
 634 N<sub>2</sub>O Release and on the Community Structure of Ammonia Oxidizers and Denitrifiers,  
 635 *Applied and Environmental Microbiology*, 68, 5685–5692,  
 636 <https://doi.org/10.1128/AEM.68.11.5685-5692.2002>, 2002.

637 Balderston, W. L., Sherr, B., and Payne, W. J.: Blockage by acetylene of nitrous oxide  
 638 reduction in *Pseudomonas perfectomarinus*, *Applied and Environmental Microbiology*,  
 639 31, 504–508, <https://doi.org/10.1128/aem.31.4.504-508.1976>, 1976.

640 Bateman, E. J. and Baggs, E. M.: Contributions of nitrification and denitrification to N<sub>2</sub>O  
 641 emissions from soils at different water-filled pore space, *Biology and Fertility of Soils*,  
 642 41, 379–388, <https://doi.org/10.1007/s00374-005-0858-3>, 2005.

643 Cao, X. and Liu, Y.: Equilibrium mass-dependent fractionation relationships for triple  
 644 oxygen isotopes, *Geochimica et Cosmochimica Acta*, 75, 7435–7445,  
 645 <https://doi.org/10.1016/j.gca.2011.09.048>, 2011.

646 Chen, G. C., Tam, N. F. Y., and Ye, Y.: Spatial and seasonal variations of atmospheric  
 647 N<sub>2</sub>O and CO<sub>2</sub> fluxes from a subtropical mangrove swamp and their relationships with soil  
 648 characteristics, *Soil Biology and Biochemistry*, 48, 175–181,  
 649 <https://doi.org/10.1016/j.soilbio.2012.01.029>, 2012.

650 Choudhary, M. A., Akramkhanov, A., and Saggar, S.: Nitrous oxide emissions from a  
 651 New Zealand cropped soil: tillage effects, spatial and seasonal variability, *Agriculture,  
 652 Ecosystems & Environment*, 93, 33–43, [https://doi.org/10.1016/S0167-8809\(02\)00005-1](https://doi.org/10.1016/S0167-8809(02)00005-1),  
 653 2002.

654 Cliff, S. S., Brenninkmeijer, C. A. M., and Thiemens, M. H.: First measurement of the  
 655 <sup>18</sup>O/<sup>16</sup>O and <sup>17</sup>O/<sup>16</sup>O ratios in stratospheric nitrous oxide: A mass-independent anomaly,

Journal of Geophysical Research: Atmospheres, 104, 16171–16175,  
<https://doi.org/10.1029/1999JD900152>, 1999.

Decock, C. and Six, J.: An assessment of N-cycling and sources of N<sub>2</sub>O during a simulated rain event using natural abundance <sup>15</sup>N, Agriculture, Ecosystems & Environment, 165, 141–150, <https://doi.org/10.1016/j.agee.2012.11.012>, 2013.

Dickinson, R. E. and Cicerone, R. J.: Future global warming from atmospheric trace gases, Nature, 319, 109–115, <https://doi.org/10.1038/319109a0>, 1986.

Ding, W., Tsunogai, U., Nakagawa, F., Sambuichi, T., Sase, H., Morohashi, M., and Yotsuyanagi, H.: Tracing the source of nitrate in a forested stream showing elevated concentrations during storm events, Biogeosciences, 19, 3247–3261, <https://doi.org/10.5194/bg-19-3247-2022>, 2022.

Ding, W., Tsunogai, U., Nakagawa, F., Sambuichi, T., Chiwa, M., Kasahara, T., and Shinozuka, K.: Stable isotopic evidence for the excess leaching of unprocessed atmospheric nitrate from forested catchments under high nitrogen saturation, Biogeosciences, 20, 753–766, <https://doi.org/10.5194/bg-20-753-2023>, 2023.

Ding, W., Tsunogai, U., and Nakagawa, F.: Bias in calculating gross nitrification rates in forested catchments using the triple oxygen isotopic composition ( $\Delta^{17}\text{O}$ ) of stream nitrate, Biogeosciences, 21, 4717–4722, <https://doi.org/10.5194/bg-21-4717-2024>, 2024.

Hattori, S., Nuñez Palma, Y., Itoh, Y., Kawasaki, M., Fujihara, Y., Takase, K., and Yoshida, N.: Isotopic evidence for seasonality of microbial internal nitrogen cycles in a temperate forested catchment with heavy snowfall, Science of The Total Environment, 690, 290–299, <https://doi.org/10.1016/j.scitotenv.2019.06.507>, 2019.

Hirota, A., Tsunogai, U., Komatsu, D. D., and Nakagawa, F.: Simultaneous determination of  $\delta^{15}\text{N}$  and  $\delta^{18}\text{O}$  of N<sub>2</sub>O and  $\delta^{13}\text{C}$  of CH<sub>4</sub> in nanomolar quantities from a single water sample, Rapid Communications in Mass Spectrometry, 24, 1085–1092, <https://doi.org/10.1002/rcm.4483>, 2010.

Hiyama, T., Kochi, K., Kobayashi, N., and Sirisampan, S.: Seasonal variation in stomatal conductance and physiological factors observed in a secondary warm-temperate forest, Ecological Research, 20, 333–346, <https://doi.org/10.1007/s11284-005-0049-6>, 2005.

Homyak, P. M., Vasquez, K. T., Sickman, J. O., Parker, D. R., and Schimel, J. P.: Improving Nitrite Analysis in Soils: Drawbacks of the Conventional 2 M KCl Extraction, Soil Science Society of America Journal, 79, 1237–1242, <https://doi.org/10.2136/sssaj2015.02.0061n>, 2015.

Ibraim, E., Wolf, B., Harris, E., Gasche, R., Wei, J., Yu, L., Kiese, R., Eggleston, S., Butterbach-Bahl, K., Zeeman, M., Tuzson, B., Emmenegger, L., Six, J., Henne, S., and Mohn, J.: Attribution of N<sub>2</sub>O sources in a grassland soil with laser spectroscopy based

isotopocule analysis, *Biogeosciences*, 16, 3247–3266, <https://doi.org/10.5194/bg-16-3247-2019>, 2019.

Kaiser, J., Röckmann, T., and Brenninkmeijer, C. A. M.: Complete and accurate mass spectrometric isotope analysis of tropospheric nitrous oxide, *Journal of Geophysical Research: Atmospheres*, 108, <https://doi.org/10.1029/2003JD003613>, 2003.

Kaiser, J., Hastings, M. G., Houlton, B. Z., Röckmann, T., and Sigman, D. M.: Triple Oxygen Isotope Analysis of Nitrate Using the Denitrifier Method and Thermal Decomposition of  $\text{N}_2\text{O}$ , *Analytical Chemistry*, 79, 599–607, <https://doi.org/10.1021/ac061022s>, 2007.

Kaushal, R., Hsueh, Y.-H., Chen, C.-L., Lan, Y.-P., Wu, P.-Y., Chen, Y.-C., and Liang, M.-C.: Isotopic assessment of soil  $\text{N}_2\text{O}$  emission from a sub-tropical agricultural soil under varying N-inputs, *Science of The Total Environment*, 827, 154311, <https://doi.org/10.1016/j.scitotenv.2022.154311>, 2022.

Keeling, C. D.: The concentration and isotopic abundances of atmospheric carbon dioxide in rural areas, *Geochimica et Cosmochimica Acta*, 13, 322–334, [https://doi.org/10.1016/0016-7037\(58\)90033-4](https://doi.org/10.1016/0016-7037(58)90033-4), 1958.

Khalil, K., Mary, B., and Renault, P.: Nitrous oxide production by nitrification and denitrification in soil aggregates as affected by  $\text{O}_2$  concentration, *Soil Biology and Biochemistry*, 36, 687–699, <https://doi.org/10.1016/j.soilbio.2004.01.004>, 2004.

Kim, K.-R. and Craig, H.: Nitrogen-15 and Oxygen-18 Characteristics of Nitrous Oxide: A Global Perspective, *Science*, 262, 1855–1857, <https://doi.org/10.1126/science.262.5141.1855>, 1993.

Komatsu, D. D., Ishimura, T., Nakagawa, F., and Tsunogai, U.: Determination of the  $^{15}\text{N}/^{14}\text{N}$ ,  $^{17}\text{O}/^{16}\text{O}$ , and  $^{18}\text{O}/^{16}\text{O}$  ratios of nitrous oxide by using continuous-flow isotope-ratio mass spectrometry, *Rapid Communications in Mass Spectrometry*, 22, 1587–1596, <https://doi.org/10.1002/rcm.3493>, 2008.

Kool, D. M., Wrage, N., Oenema, O., Dolfing, J., and Van Groenigen, J. W.: Oxygen exchange between (de)nitrification intermediates and  $\text{H}_2\text{O}$  and its implications for source determination of  $\text{NO}$  and  $\text{N}_2\text{O}$ : a review, *Rapid Communications in Mass Spectrometry*, 21, 3569–3578, <https://doi.org/10.1002/rcm.3249>, 2007.

Kool, D. M., Dolfing, J., Wrage, N., and Van Groenigen, J. W.: Nitrifier denitrification as a distinct and significant source of nitrous oxide from soil, *Soil Biology and Biochemistry*, 43, 174–178, <https://doi.org/10.1016/j.soilbio.2010.09.030>, 2011.

Lewicka-Szczebak, D., Well, R., Köster, J. R., Fuß, R., Senbayram, M., Dittert, K., and Flessa, H.: Experimental determinations of isotopic fractionation factors associated with  $\text{N}_2\text{O}$  production and reduction during denitrification in soils, *Geochimica et Cosmochimica Acta*, 134, 55–73, <https://doi.org/10.1016/j.gca.2014.03.010>, 2014.

Lewicka-Szczebak, D., Well, R., Bol, R., Gregory, A. S., Matthews, G. P., Misselbrook, T., Whalley, W. R., and Cardenas, L. M.: Isotope fractionation factors controlling

731 isotopocule signatures of soil-emitted N<sub>2</sub>O produced by denitrification processes of  
732 various rates, *Rapid Communications in Mass Spectrometry*, 29, 269–282,  
733 <https://doi.org/10.1002/rcm.7102>, 2015.

734 Lewicka-Szczebak, D., Jansen-Willems, A., Müller, C., Dyckmans, J., and Well, R.:  
735 Nitrite isotope characteristics and associated soil N transformations, *Scientific Reports*,  
736 11, 5008, <https://doi.org/10.1038/s41598-021-83786-w>, 2021.

737 Lin, W., Ding, J., Li, Y., Zhang, W., Ahmad, R., Xu, C., Mao, L., Qiang, X., Zheng, Q.,  
738 and Li, Q.: Partitioning of sources of N<sub>2</sub>O from soil treated with different types of  
739 fertilizers by the acetylene inhibition method and stable isotope analysis, *European*  
740 *Journal of Soil Science*, 70, 1037–1048, <https://doi.org/10.1111/ejss.12782>, 2019.

741 Luo, J., Ledgard, S. F., and Lindsey, S. B.: Nitrous oxide emissions from application of  
742 urea on New Zealand pasture, *New Zealand Journal of Agricultural Research*, 50, 1–11,  
743 <https://doi.org/10.1080/00288230709510277>, 2007.

744 Lyu, S.: Variability of  $\delta^2\text{H}$  and  $\delta^{18}\text{O}$  in Soil Water and Its Linkage to Precipitation in an  
745 East Asian Monsoon Subtropical Forest Plantation, *Water*, 13, 2930,  
746 <https://doi.org/10.3390/w13202930>, 2021.

747 Mathieu, O., Hénault, C., Lévêque, J., Baujard, E., Milloux, M.-J., and Andreux, F.:  
748 Quantifying the contribution of nitrification and denitrification to the nitrous oxide flux  
749 using <sup>15</sup>N tracers, *Environmental Pollution*, 144, 933–940,  
750 <https://doi.org/10.1016/j.envpol.2006.02.005>, 2006.

751 Matsuhisa, Y., Goldsmith, J. R., and Clayton, R. N.: Mechanisms of hydrothermal  
752 crystallization of quartz at 250 °C and 15 kbar, *Geochimica et Cosmochimica Acta*, 42,  
753 173–182, [https://doi.org/10.1016/0016-7037\(78\)90130-8](https://doi.org/10.1016/0016-7037(78)90130-8), 1978.

754 McIlvin, M. R. and Altabet, M. A.: Chemical Conversion of Nitrate and Nitrite to Nitrous  
755 Oxide for Nitrogen and Oxygen Isotopic Analysis in Freshwater and Seawater, *Analytical*  
756 *Chemistry*, 77, 5589–5595, <https://doi.org/10.1021/ac050528s>, 2005.

757 McKenney, D. J., Wade, D. L., and Findlay, W. I.: Rates of N<sub>2</sub>O evolution from N-  
758 fertilized soil, *Geophysical Research Letters*, 5, 777–780,  
759 <https://doi.org/10.1029/GL005i009p00777>, 1978.

760 Michalski, G., Böhlke, J. K., and Thiemens, M.: Long term atmospheric deposition as the  
761 source of nitrate and other salts in the Atacama Desert, Chile: New evidence from mass-  
762 independent oxygen isotopic compositions, *Geochimica et Cosmochimica Acta*, 68,  
763 4023–4038, <https://doi.org/10.1016/j.gca.2004.04.009>, 2004.

764 Miller, M. F.: Isotopic fractionation and the quantification of <sup>17</sup>O anomalies in the oxygen  
765 three-isotope system: an appraisal and geochemical significance, *Geochimica et*



766 Cosmochimica Acta, 66, 1881–1889, [https://doi.org/10.1016/S0016-7037\(02\)00832-3](https://doi.org/10.1016/S0016-7037(02)00832-3),  
767 2002.

768 Mulvaney, R. L. and Kurtz, L. T.: A New Method for Determination of  $^{15}\text{N}$ -Labeled  
769 Nitrous Oxide, Soil Science Soc of Amer J, 46, 1178–1184,  
770 <https://doi.org/10.2136/sssaj1982.03615995004600060012x>, 1982.

771 Nakagawa, F., Tsunogai, U., Obata, Y., Ando, K., Yamashita, N., Saito, T., Uchiyama,  
772 S., Morohashi, M., and Sase, H.: Export flux of unprocessed atmospheric nitrate from  
773 temperate forested catchments: a possible new index for nitrogen saturation,  
774 Biogeosciences, 15, 7025–7042, <https://doi.org/10.5194/bg-15-7025-2018>, 2018.

775 Okabe, S., Oshiki, M., Takahashi, Y., and Satoh, H.:  $\text{N}_2\text{O}$  emission from a partial  
776 nitrification–anammox process and identification of a key biological process of  $\text{N}_2\text{O}$   
777 emission from anammox granules, Water Research, 45, 6461–6470,  
778 <https://doi.org/10.1016/j.watres.2011.09.040>, 2011.

779 Opdyke, M. R., Ostrom, N. E., and Ostrom, P. H.: Evidence for the predominance of  
780 denitrification as a source of  $\text{N}_2\text{O}$  in temperate agricultural soils based on isotopologue  
781 measurements, Global Biogeochemical Cycles, 23,  
782 <https://doi.org/10.1029/2009GB003523>, 2009.

783 Ostrom, N. E., Pitt, A., Sutka, R., Ostrom, P. H., Grandy, A. S., Huizinga, K. M., and  
784 Robertson, G. P.: Isotopologue effects during  $\text{N}_2\text{O}$  reduction in soils and in pure cultures  
785 of denitrifiers, Journal of Geophysical Research: Biogeosciences, 112,  
786 <https://doi.org/10.1029/2006JG000287>, 2007.

787 Pack, A. and Herwartz, D.: The triple oxygen isotope composition of the Earth mantle  
788 and understanding  $\Delta^{17}\text{O}$  variations in terrestrial rocks and minerals, Earth and Planetary  
789 Science Letters, 390, 138–145, <https://doi.org/10.1016/j.epsl.2014.01.017>, 2014.

790 Sambuichi, T., Tsunogai, U., Kura, K., Nakagawa, F., and Ohba, T.: High-precision  
791  $\Delta^{17}\text{O}$  measurements of geothermal  $\text{H}_2\text{O}$  and MORB on the VSMOW-SLAP scale:  
792 evidence for active oxygen exchange between the lithosphere and hydrosphere,  
793 Geochemical Journal, 55, e25–e33, <https://doi.org/10.2343/geochemj.2.0644>, 2021.

794 Sambuichi, T., Tsunogai, U., Ito, M., and Nakagawa, F.: First Measurements on Triple  
795 Oxygen Isotopes of Dissolved Inorganic Phosphate in the Hydrosphere, Environmental  
796 Science and Technology, 57, 3415–3424, <https://doi.org/10.1021/acs.est.2c08520>, 2023.

797 Sharp, Z. D. and Wostbrock, J. A. G.: Standardization for the Triple Oxygen Isotope  
798 System: Waters, Silicates, Carbonates, Air, and Sulfates, Reviews in Mineralogy and  
799 Geochemistry, 86, 179–196, <https://doi.org/10.2138/rmg.2021.86.05>, 2021.

800 Sharp, Z. D., Gibbons, J. A., Maltsev, O., Atudorei, V., Pack, A., Sengupta, S., Shock,  
801 E. L., and Knauth, L. P.: A calibration of the triple oxygen isotope fractionation in the

802 SiO<sub>2</sub>–H<sub>2</sub>O system and applications to natural samples, *Geochimica et Cosmochimica*  
803 *Acta*, 186, 105–119, <https://doi.org/10.1016/j.gca.2016.04.047>, 2016.

804 Shen, Q. R., Ran, W., and Cao, Z. H.: Mechanisms of nitrite accumulation occurring in  
805 soil nitrification, *Chemosphere*, 50, 747–753, [https://doi.org/10.1016/S0045-](https://doi.org/10.1016/S0045-6535(02)00215-1)  
806 6535(02)00215-1, 2003.

807 Snider, D. M., Schiff, S. L., and Spoelstra, J.: <sup>15</sup>N/<sup>14</sup>N and <sup>18</sup>O/<sup>16</sup>O stable isotope ratios of  
808 nitrous oxide produced during denitrification in temperate forest soils, *Geochimica et*  
809 *Cosmochimica Acta*, 73, 877–888, <https://doi.org/10.1016/j.gca.2008.11.004>, 2009.

810 Takahashi, K.: Oxygen isotope ratios between soil water and stem water of trees in pot  
811 experiments, *Ecological Research*, 13, 1–5, [https://doi.org/10.1046/j.1440-](https://doi.org/10.1046/j.1440-1703.1998.00240.x)  
812 1703.1998.00240.x, 1998.

813 Tang, C.-J., Zheng, P., Wang, C.-H., Mahmood, Q., Zhang, J.-Q., Chen, X.-G., Zhang,  
814 L., and Chen, J.-W.: Performance of high-loaded ANAMMOX UASB reactors  
815 containing granular sludge, *Water Research*, 45, 135–144,  
816 <https://doi.org/10.1016/j.watres.2010.08.018>, 2011.

817 Thiemens, M. H. and Trogler, W. C.: Nylon Production: An Unknown Source of  
818 Atmospheric Nitrous Oxide, *Science*, 251, 932–934,  
819 <https://doi.org/10.1126/science.251.4996.932>, 1991.

820 Tian, H., Xu, R., Canadell, J. G., Thompson, R. L., Winiwarter, W., Suntharalingam, P.,  
821 Davidson, E. A., Ciais, P., Jackson, R. B., Janssens-Maenhout, G., Prather, M. J.,  
822 Regnier, P., Pan, N., Pan, S., Peters, G. P., Shi, H., Tubiello, F. N., Zaehle, S., Zhou, F.,  
823 Arneeth, A., Battaglia, G., Berthet, S., Bopp, L., Bouwman, A. F., Buitenhuis, E. T.,  
824 Chang, J., Chipperfield, M. P., Dangal, S. R. S., Dlugokencky, E., Elkins, J. W., Eyre, B.  
825 D., Fu, B., Hall, B., Ito, A., Joos, F., Krummel, P. B., Landolfi, A., Laruelle, G. G.,  
826 Lauerwald, R., Li, W., Lienert, S., Maavara, T., MacLeod, M., Millet, D. B., Olin, S.,  
827 Patra, P. K., Prinn, R. G., Raymond, P. A., Ruiz, D. J., van der Werf, G. R., Vuichard, N.,  
828 Wang, J., Weiss, R. F., Wells, K. C., Wilson, C., Yang, J., and Yao, Y.: A comprehensive  
829 quantification of global nitrous oxide sources and sinks, *Nature*, 586, 248–256,  
830 <https://doi.org/10.1038/s41586-020-2780-0>, 2020.

831 Toyoda, S., Yano, M., Nishimura, S., Akiyama, H., Hayakawa, A., Koba, K., Sudo, S.,  
832 Yagi, K., Makabe, A., Tobari, Y., Ogawa, N. O., Ohkouchi, N., Yamada, K., and  
833 Yoshida, N.: Characterization and production and consumption processes of N<sub>2</sub>O emitted  
834 from temperate agricultural soils determined via isotopomer ratio analysis, *Global*  
835 *Biogeochemical Cycles*, 25, <https://doi.org/10.1029/2009GB003769>, 2011.

836 Toyoda, S., Kuroki, N., Yoshida, N., Ishijima, K., Tohjima, Y., and Machida, T.: Decadal  
837 time series of tropospheric abundance of N<sub>2</sub>O isotopomers and isotopologues in the  
838 Northern Hemisphere obtained by the long-term observation at Hateruma Island, Japan,

839 Journal of Geophysical Research: Atmospheres, 118, 3369–3381,  
840 <https://doi.org/10.1002/jgrd.50221>, 2013.

841 Toyoda, S., Yoshida, N., and Koba, K.: Isotopocule analysis of biologically produced  
842 nitrous oxide in various environments, *Mass Spectrometry Reviews*, 36, 135–160,  
843 <https://doi.org/10.1002/mas.21459>, 2017.

844 Tsunogai, U., Ishibashi, J., Wakita, H., and Gamo, T.: Methane-rich plumes in the Suruga  
845 Trough (Japan) and their carbon isotopic characterization, *Earth and Planetary Science*  
846 *Letters*, 160, 97–105, [https://doi.org/10.1016/S0012-821X\(98\)00075-2](https://doi.org/10.1016/S0012-821X(98)00075-2), 1998.

847 Tsunogai, U., Hachisu, Y., Komatsu, D. D., Nakagawa, F., Gamo, T., and Akiyama, K.:  
848 An updated estimation of the stable carbon and oxygen isotopic compositions of  
849 automobile CO emissions, *Atmospheric Environment*, 37, 4901–4910,  
850 <https://doi.org/10.1016/j.atmosenv.2003.08.008>, 2003.

851 Tsunogai, U., Kido, T., Hirota, A., Ohkubo, S. B., Komatsu, D. D., and Nakagawa, F.:  
852 Sensitive determinations of stable nitrogen isotopic composition of organic nitrogen  
853 through chemical conversion into N<sub>2</sub>O, *Rapid Communications in Mass Spectrometry*,  
854 22, 345–354, <https://doi.org/10.1002/rcm.3368>, 2008.

855 Tsunogai, U., Komatsu, D. D., Daita, S., Kazemi, G. A., Nakagawa, F., Noguchi, I., and  
856 Zhang, J.: Tracing the fate of atmospheric nitrate deposited onto a forest ecosystem in  
857 Eastern Asia using  $\Delta^{17}\text{O}$ , *Atmospheric Chemistry and Physics*, 10, 1809–1820,  
858 <https://doi.org/10.5194/acp-10-1809-2010>, 2010.

859 Tsunogai, U., Kamimura, K., Anzai, S., Nakagawa, F., and Komatsu, D. D.: Hydrogen  
860 isotopes in volcanic plumes: Tracers for remote temperature sensing of fumaroles,  
861 *Geochimica et Cosmochimica Acta*, 75, 4531–4546,  
862 <https://doi.org/10.1016/j.gca.2011.05.023>, 2011.

863 Tsushima, I., Ogasawara, Y., Kindaichi, T., Satoh, H., and Okabe, S.: Development of  
864 high-rate anaerobic ammonium-oxidizing (anammox) biofilm reactors, *Water Research*,  
865 41, 1623–1634, <https://doi.org/10.1016/j.watres.2007.01.050>, 2007.

866 Uechi, Y. and Uemura, R.: Dominant influence of the humidity in the moisture source  
867 region on the  $^{17}\text{O}$ -excess in precipitation on a subtropical island, *Earth and Planetary*  
868 *Science Letters*, 513, 20–28, <https://doi.org/10.1016/j.epsl.2019.02.012>, 2019.

869 Verhoeven, E., Barthel, M., Yu, L., Celi, L., Said-Pullicino, D., Sleutel, S., Lewicka-  
870 Szczebak, D., Six, J., and Decock, C.: Early season N<sub>2</sub>O emissions under variable water  
871 management in rice systems: source-partitioning emissions using isotope ratios along a  
872 depth profile, *Biogeosciences*, 16, 383–408, <https://doi.org/10.5194/bg-16-383-2019>,  
873 2019.

874 Wankel, S. D., Ziebis, W., Buchwald, C., Charoenpong, C., de Beer, D., Dentinger, J.,  
875 Xu, Z., and Zengler, K.: Evidence for fungal and chemodenitrification based N<sub>2</sub>O flux

876 from nitrogen impacted coastal sediments, *Nature Communication*, 8, 15595,  
877 <https://doi.org/10.1038/ncomms15595>, 2017.

878 WMO.: WMO greenhouse gas bulletin (GHG Bulletin), Assessed from:  
879 <https://library.wmo.int/records/item/68532-no-19-15-november-2023>, 2023.

880 Wrage, N., Velthof, G. L., van Beusichem, M. L., and Oenema, O.: Role of nitrifier  
881 denitrification in the production of nitrous oxide, *Soil Biology and Biochemistry*, 33,  
882 1723–1732, [https://doi.org/10.1016/S0038-0717\(01\)00096-7](https://doi.org/10.1016/S0038-0717(01)00096-7), 2001.

883 Wrage, N., Lauf, J., del Prado, A., Pinto, M., Pietrzak, S., Yamulki, S., Oenema, O., and  
884 Gebauer, G.: Distinguishing sources of N<sub>2</sub>O in European grasslands by stable isotope  
885 analysis, *Rapid Communications in Mass Spectrometry*, 18, 1201–1207,  
886 <https://doi.org/10.1002/rcm.1461>, 2004.

887 Wrage, N., Groenigen, J. W. van, Oenema, O., and Baggs, E. M.: A novel dual-isotope  
888 labelling method for distinguishing between soil sources of N<sub>2</sub>O, *Rapid Communications*  
889 *in Mass Spectrometry*, 19, 3298–3306, <https://doi.org/10.1002/rcm.2191>, 2005.

890 Xu, H., Tsunogai, U., Nakagawa, F., Li, Y., Ito, M., Sato, K., and Tanimoto, H.:  
891 Determination of the triple oxygen isotopic composition of tropospheric ozone in  
892 terminal positions using a multistep nitrite-coated filter-pack system, *Rapid*  
893 *Communications in Mass Spectrometry*, 35, e9124, <https://doi.org/10.1002/rcm.9124>,  
894 2021.

895 Yan, Y., Sha, L., Cao, M., Zheng, Z., Tang, J., Wang, Y., Zhang, Y., Wang, R., Liu, G.,  
896 Wang, Y., and Sun, Y.: Fluxes of CH<sub>4</sub> and N<sub>2</sub>O from soil under a tropical seasonal rain  
897 forest in Xishuangbanna, Southwest China, *Journal of Environmental Sciences*, 20, 207–  
898 215, [https://doi.org/10.1016/S1001-0742\(08\)60033-9](https://doi.org/10.1016/S1001-0742(08)60033-9), 2008.

899 York, D., Evensen, N. M., Martínez, M. L., and De Basabe Delgado, J.: Unified  
900 equations for the slope, intercept, and standard errors of the best straight line, *American*  
901 *Journal of Physics*, 72, 367–375, <https://doi.org/10.1119/1.1632486>, 2004.

902 Young, E. D., Galy, A., and Nagahara, H.: Kinetic and equilibrium mass-dependent  
903 isotope fractionation laws in nature and their geochemical and cosmochemical  
904 significance, *Geochimica et Cosmochimica Acta*, 66, 1095–1104,  
905 [https://doi.org/10.1016/S0016-7037\(01\)00832-8](https://doi.org/10.1016/S0016-7037(01)00832-8), 2002.

906 Yu, L., Harris, E., Lewicka-Szczebak, D., Barthel, M., Blomberg, M. R. A., Harris, S. J.,  
907 Johnson, M. S., Lehmann, M. F., Liisberg, J., Müller, C., Ostrom, N. E., Six, J., Toyoda,  
908 S., Yoshida, N., and Mohn, J.: What can we learn from N<sub>2</sub>O isotope data? – Analytics,

909 processes and modelling, *Rapid Communications in Mass Spectrometry*, 34, e8858,  
910 <https://doi.org/10.1002/rcm.8858>, 2020.

911 Zhang, W., Li, Y., Xu, C., Li, Q., and Lin, W.: Isotope signatures of N<sub>2</sub>O emitted from  
912 vegetable soil: Ammonia oxidation drives N<sub>2</sub>O production in NH<sub>4</sub><sup>+</sup>-fertilized soil of  
913 North China, *Scientific Reports*, 6, 29257, <https://doi.org/10.1038/srep29257>, 2016.

914 Zhu, G., Wang, S., Wang, Y., Wang, C., Risgaard-Petersen, N., Jetten, M. S., and Yin,  
915 C.: Anaerobic ammonia oxidation in a fertilized paddy soil, *ISME Journal*, 5, 1905–1912,  
916 <https://doi.org/10.1038/ismej.2011.63>, 2011.

917 Zhu, X., Burger, M., Doane, T. A., and Horwath, W. R.: Ammonia oxidation pathways  
918 and nitrifier denitrification are significant sources of N<sub>2</sub>O and NO under low oxygen  
919 availability, *Proceedings of the National Academy of Sciences*, 110, 6328–6333,  
920 <https://doi.org/10.1073/pnas.1219993110>, 2013.

921 Zou, Y., Hirono, Y., Yanai, Y., Hattori, S., Toyoda, S., and Yoshida, N.: Rainwater, soil  
922 water, and soil nitrate effects on oxygen isotope ratios of nitrous oxide produced in a  
923 green tea (*Camellia sinensis*) field in Japan, *Rapid Communications in Mass*  
924 *Spectrometry*, 29, 891–900, <https://doi.org/10.1002/rcm.7176>, 2015.

925

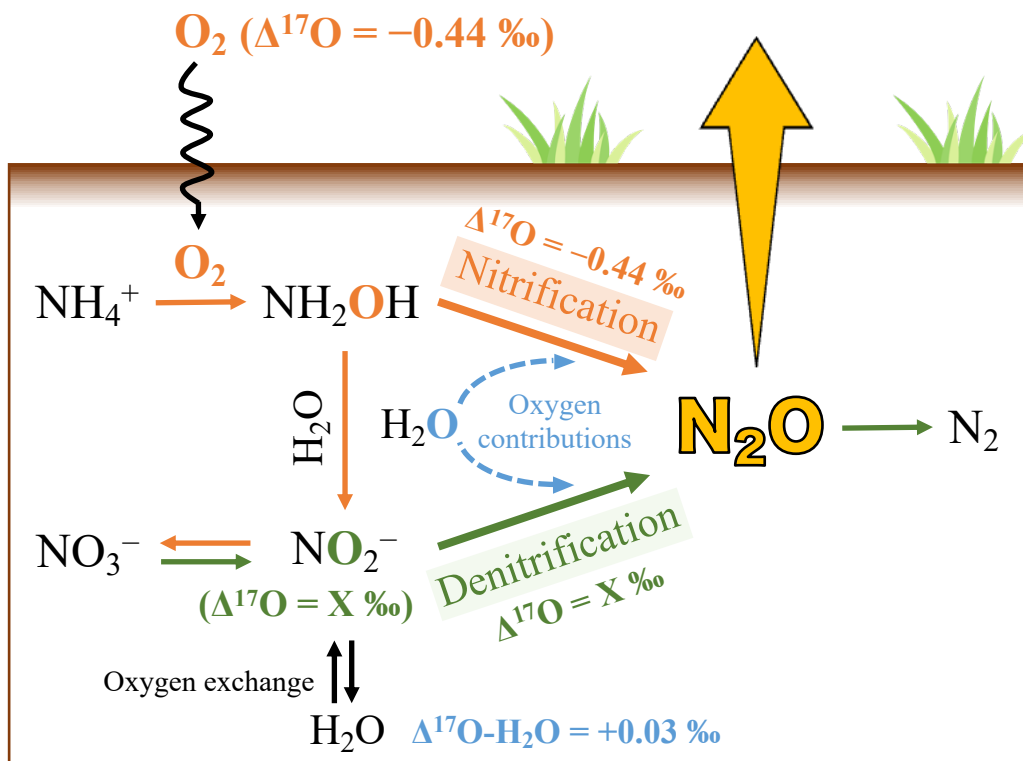


**Figure 1.** Schematic showing the pathways of  $\text{N}_2\text{O}$  production in soil (Kool et al., 2007, 2011; Wankel et al., 2017; Wrage et al., 2005) and the  $\Delta^{17}\text{O}$  values of  $\text{O}_2$  (Sharp et al., 2016),  $\text{NO}_2^-$ , and  $\text{H}_2\text{O}$  (Uechi and Uemura, 2019). The orange lines, green lines, and blue dash lines indicate the processes of nitrification, denitrification, and the possible contributions of O atoms derived from soil  $\text{H}_2\text{O}$  through nitrification and denitrification, respectively.

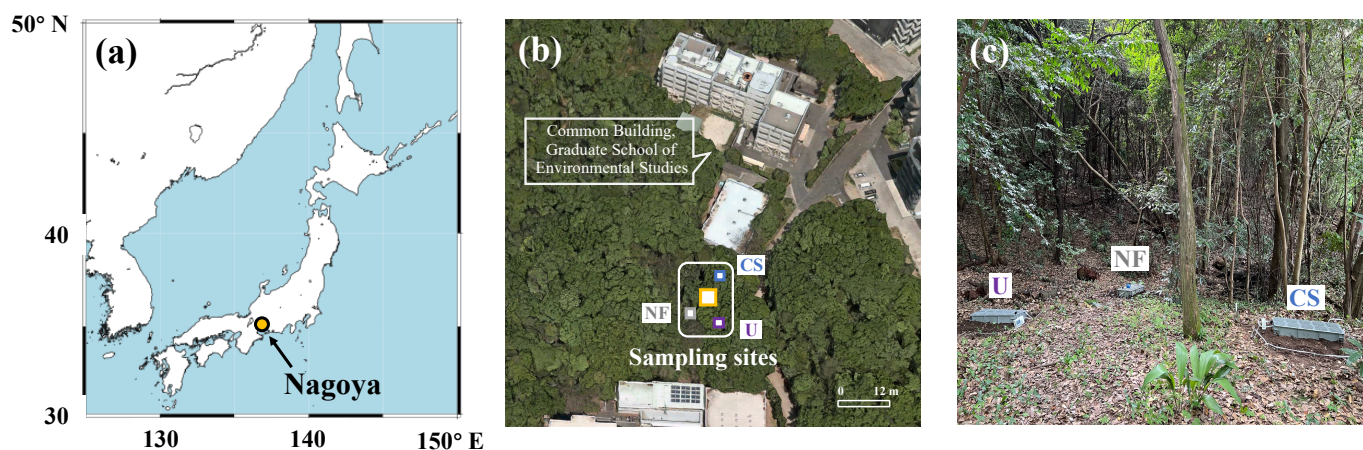


**Figure 2.** Map showing the location of Nagoya, Japan, where the studied site is located

(a). Map showing the monitoring site of  $N_2O$  emitted from forested soil in a secondary warm-temperate forest (yellow square) and the plots fertilized with Chile saltpeter (CS, blue square), urea (U, purple square), and no fertilizer (NF, gray square) (b). Photo showing the plots and flow chambers set on the plots (c).

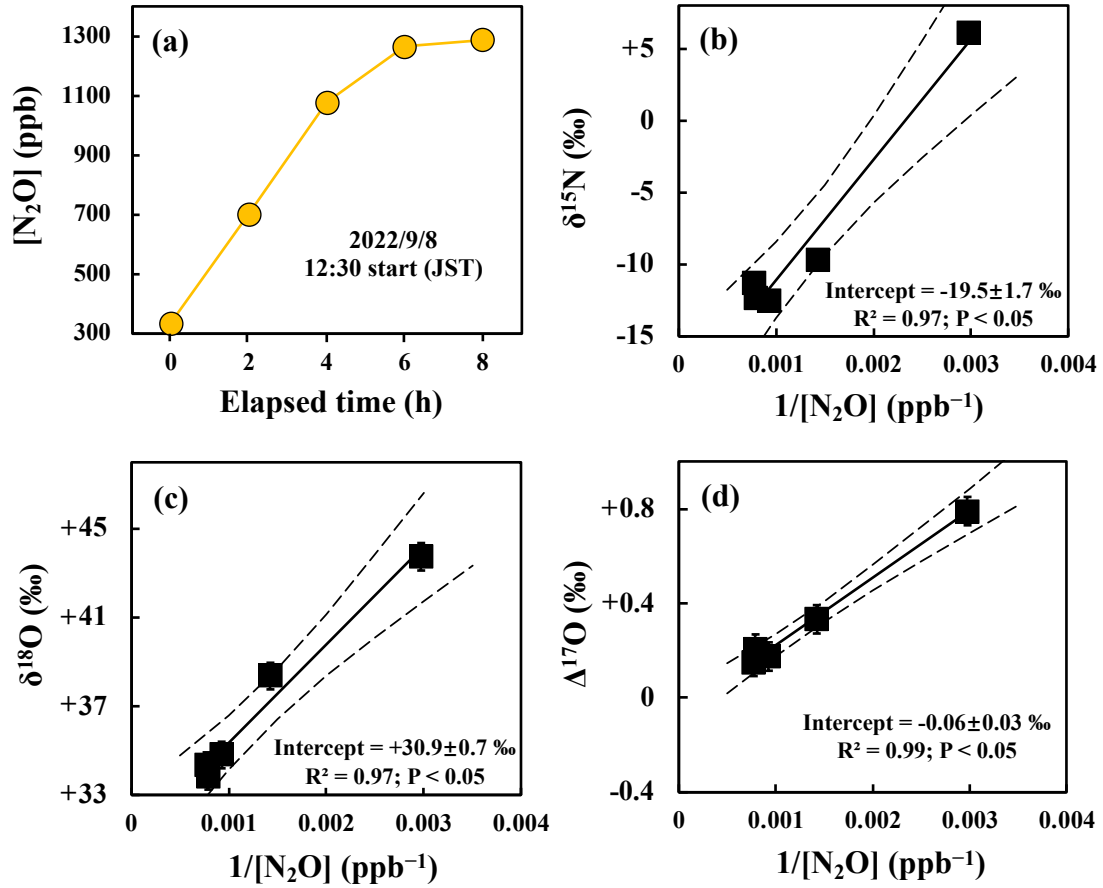
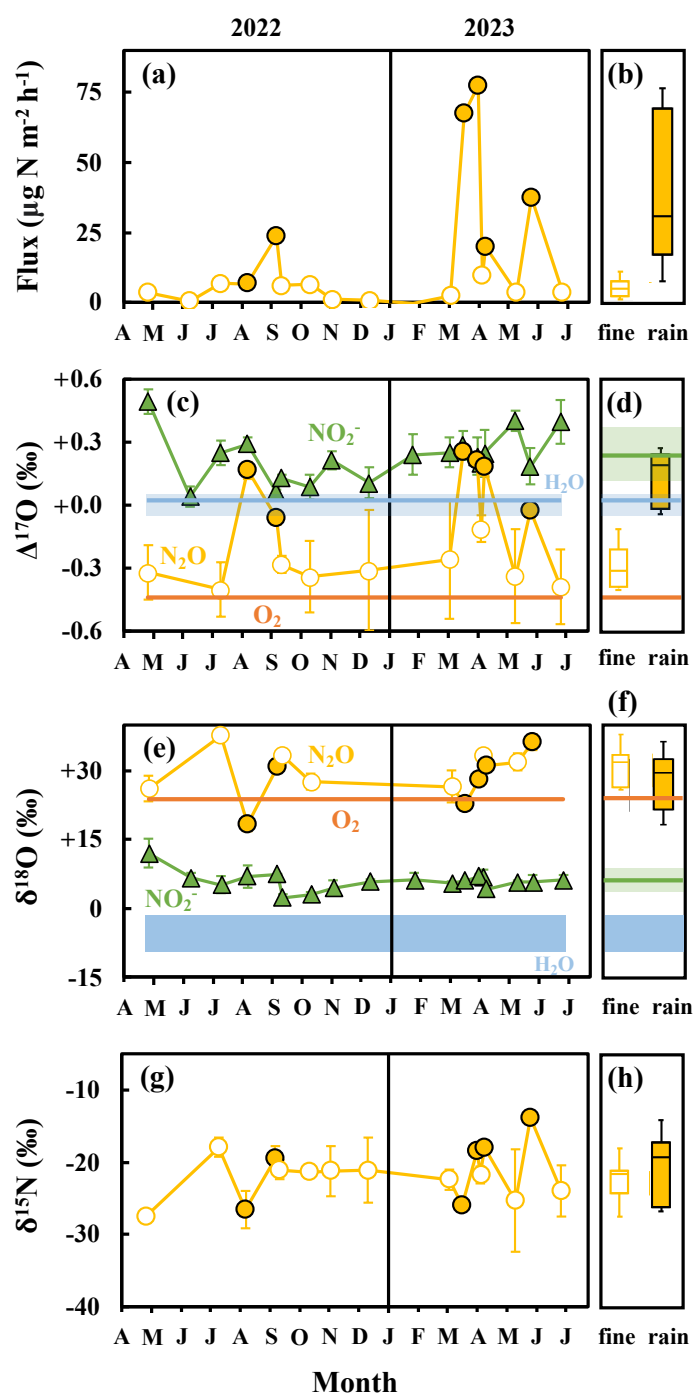


**Figure 3.** An example of changes in the concentration of  $N_2O$  ( $[N_2O]$ ) in gas samples during the observation on September 8, 2022, plotted as a function of the elapsed time since the deployment of the flow chamber on the forested soil (a), and the  $\delta^{15}N$  (b),  $\delta^{18}O$  (c), and  $\Delta^{17}O$  (d) values of  $N_2O$  plotted as a function of the reciprocal of  $[N_2O]$  ( $1/[N_2O]$ ) during the observation. Each solid line is the least squares fitting of the samples, while each dotted line is the  $2\sigma$  confidence interval of the fitting line. Error bars smaller than the sizes of the symbols are not shown.

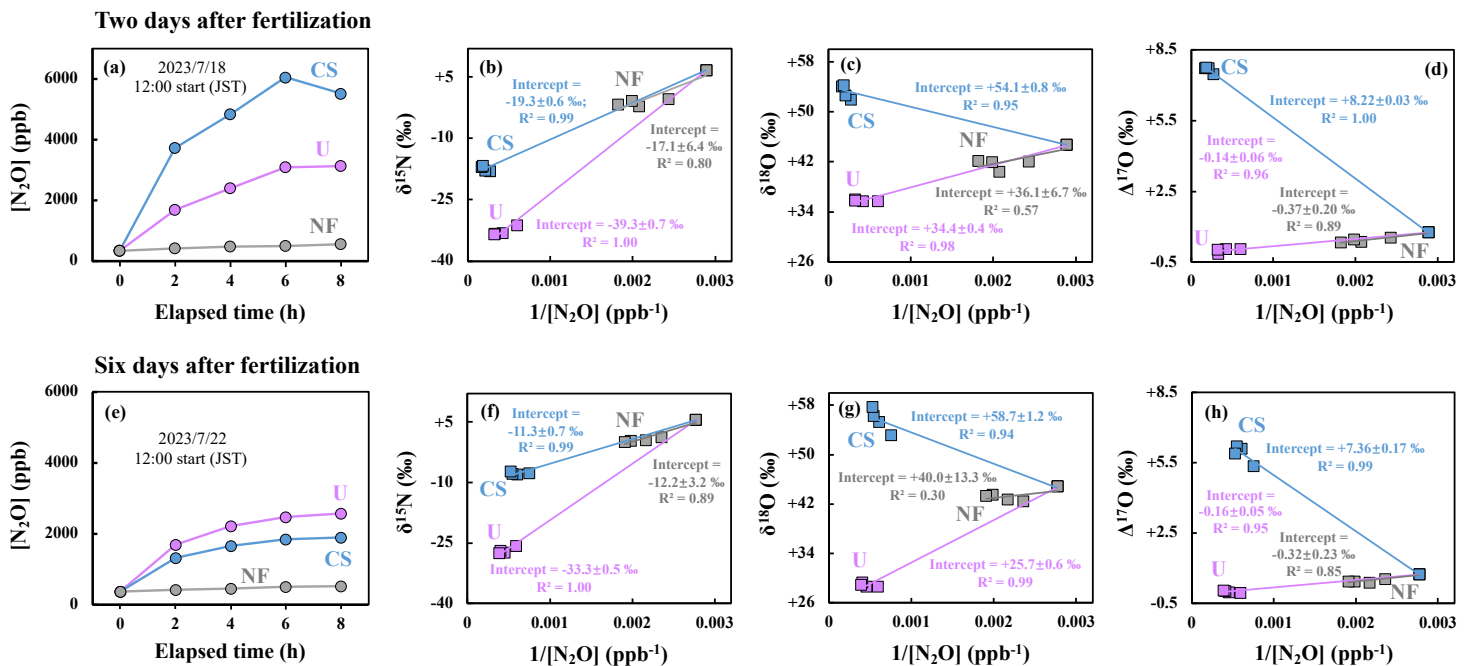




947 **Figure 4.** Temporal variations in the flux (a),  $\Delta^{17}\text{O}$  (c),  $\delta^{18}\text{O}$  (e), and  $\delta^{15}\text{N}$  (g) values of  
 948 N<sub>2</sub>O emitted from the forested soil, and the  $\delta^{18}\text{O}$  and  $\Delta^{17}\text{O}$  values of soil NO<sub>2</sub><sup>-</sup> (green  
 949 triangles), O<sub>2</sub> (orange lines), and soil H<sub>2</sub>O (blue area or line). Sampling performed on fine  
 950 and rainy days is indicated by the open (white) and solid (yellow) circles, respectively,

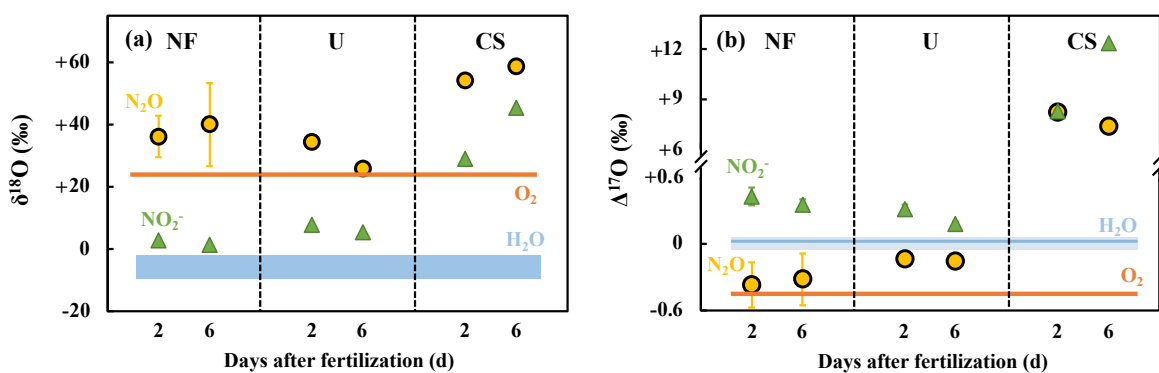
951 with the box plots of the emission flux (b),  $\Delta^{17}\text{O}$  (d),  $\delta^{18}\text{O}$  (f), and  $\delta^{15}\text{N}$  (h) of  $\text{N}_2\text{O}$  on  
 952 fine and rainy days. The black lines of the box plots indicate the median values. The  
 953 lower and upper boundaries of the box plots indicate the lower (25 %) and upper (75 %)  
 954 quartiles of data for each component, respectively. The whiskers of the box plots denote  
 955 the entire range of values for each component. Error bars smaller than the sizes of the  
 956 symbols are not shown.

957

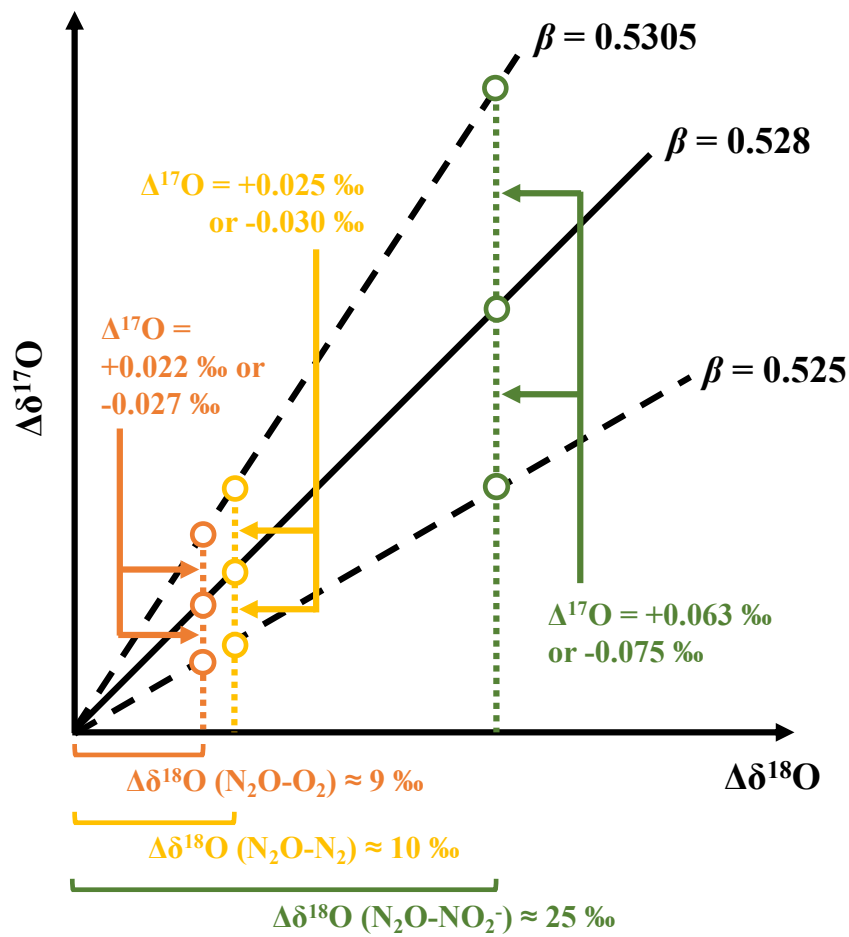


958 **Figure 5.** Changes in  $[\text{N}_2\text{O}]$  of gas samples collected from the plots of NF (gray), U  
 959 (purple), and CS (blue) 2 days after fertilization (a) and 6 days after fertilization (e) and  
 960 plotted as a function of the elapsed time since the deployment of the flow chamber; the  
 961  $\delta^{15}\text{N}$  (b and f),  $\delta^{18}\text{O}$  (c and g), and  $\Delta^{17}\text{O}$  (d and h) values of  $\text{N}_2\text{O}$  plotted as a function of  
 962 the reciprocal of  $[\text{N}_2\text{O}]$  ( $1/[\text{N}_2\text{O}]$ ). Error bars smaller than the sizes of the symbols are not  
 963 shown.

964



965 **Figure 6.** The  $\delta^{18}\text{O}$  (a) and  $\Delta^{17}\text{O}$  (b) values of  $\text{N}_2\text{O}$  (yellow circles) and  $\text{NO}_2^-$  (green  
 966 triangles) in NF, U, and CS plots determined 2 and 6 days after fertilization, and the  $\delta^{18}\text{O}$   
 967 and  $\Delta^{17}\text{O}$  values of  $\text{O}_2$  (orange lines) and soil  $\text{H}_2\text{O}$  (blue area or line). Error bars smaller  
 968 than the sizes of the symbols are not shown.



969 **Figure 7.** Schematic showing the possible variations in the  $\Delta^{17}\text{O}$  value of  $\text{N}_2\text{O}$  from that  
 970 of the source of O atoms ( $\text{O}_2$  and  $\text{NO}_2^-$ ) during transformations, including nitrification  
 971 (orange circles), denitrification (green circles), and reduction (yellow circles), due to  
 972 variations in isotope fractionation and  $\beta$  from 0.525 to 0.5305.